catalysts

MDPI

Review

SBA-15 Anchored Metal Containing Catalysts in the Oxidative Desulfurization Process

Marcello Crucianelli [1,*], Bruno Mattia Bizzarri [2] and Raffaele Saladino [2,*]

[1] Department of Physical and Chemical Sciences, University of L'Aquila, Via Vetoio, I-67100 Coppito (AQ), Italy

[2] Department of Ecology and Biology, University of Tuscia, Largo dell'Università, 01100 Viterbo (VT), Italy; bm.bizzarri@unitus.it

* Correspondence: marcello.crucianelli@univaq.it (M.C.); saladino@unitus.it (R.S.)

Received: 30 October 2019; Accepted: 18 November 2019; Published: 23 November 2019

Abstract: Recalcitrant sulfur compounds are common impurities in crude oil. During combustion they produce SO_x derivatives that are able to affect the atmospheric ozone layer, increasing the formation of acid rains, and reducing the life of the engine due to corrosion. In the last twenty years, many efforts have been devoted to develop conventional hydrodesulfurization (HDS) procedures, as well as alternative methods, such as selective adsorption, bio-desulfurization, oxidative desulfurization (ODS) under extractive conditions (ECODS), and others. Among them, the oxidative procedures have been usually accomplished by the use of toxic stoichiometric oxidants, namely potassium permanganate, sodium bromate and carboxylic and sulfonic peracids. As an alternative, increasing interest is devoted to selective and economical procedures based upon catalytic methods. Heterogeneous catalysis is of relevance in industrial ODS processes, since it reduces the leaching of active species and favors the recovery and reuse of the catalyst for successive transformations. The heterogenization of different types of high-valent metal transition-based organometallic complexes, able to promote the activation of stoichiometric benign oxidants like peroxides, can be achieved using various solid supports. Many successful cases have been frequently associated with the use of mesoporous silicas that have the advantage of easy surface modification by reaction with organosilanes, facilitating the immobilization of homogeneous catalysts. In this manuscript the application of SBA-15 as efficient support for different active metal species, able to promote the catalytic ODS of either model or real fuels is reviewed, highlighting its beneficial properties such as high surface area, narrow pore size distribution and tunable pore diameter dimensions. Related to this topic, the most relevant advances recently published, will be discussed and critically described.

Keywords: SBA-15; oxidative desulfurization; metal oxides; polyoxometalates; heterogenization

1. Introduction

Santa Barbara Amorphous (SBA) materials are mesoporous silicate-aluminosilicates characterized by uniform pore size (4.6–30 nm), well-defined pore structure and size-distribution, high surface area, high thermal stability and the capability to support a large panel of active species [1,2]. A wide variety of SBA materials has been reported in the literature like SBA-1 (Pm3n, cubic), SBA-15 (P6mm, hexagonal) and SBA-16 (Im3m, cubic) [3]. SBA-15 is one of the most promising components of this family, due to its several applications, including selective adsorption processes, heterogeneous catalysis, different chemical transformations and gas storage [4]. SBA-15 is usually prepared by supramolecular non-ionic self-assembly between ethylene oxide/propylene oxide copolymer-template (Pluronic P123) and appropriate silica precursors (tetraethoxysilane TEOS and tetramethoxysilane TMOS) in a range

of temperature from 30 °C to 120 °C, followed by calcination at high temperature to degrade the copolymer-template (Figure 1) [5,6].

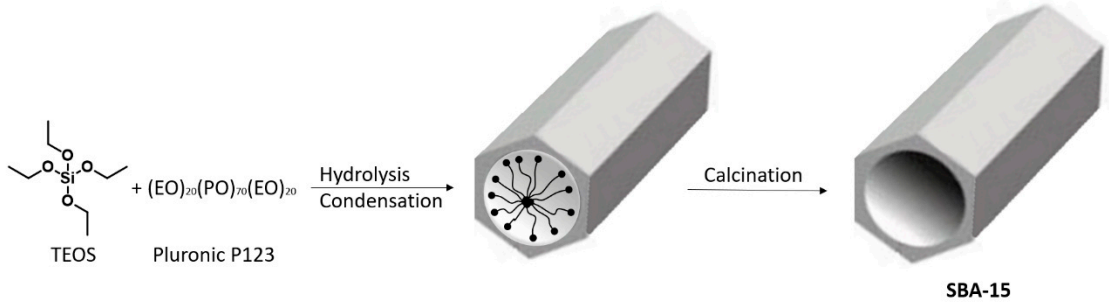

Figure 1. Sketch of the general procedure for the Santa Barbara Amorphous (SBA)-15 preparation.

In this process, the value of the ratio of ethylene oxide to propylene oxide can control the distribution function of the pores inside the basic hexagonally-arrayed channel framework. At low values of this ratio, the p6mm hexagonal morphology is favored instead of the cubic mesoporous arrangement prevailing at higher ratio values [7,8]. Alternative reaction pathways for the preparation of SBA-15 derivatives have been also reported [9–11]. SBA-15 materials have been well recognized as a promising support template for the synthesis of catalytic materials due to its uniform, hexagonally-arrayed channels with a narrow pore size distribution. These features, together with high surface area and hydrothermal stability, make it as an ideal support for the incorporation of various active molecules on its surface, provided that its mesoporous surface is previously and appropriately functionalized with various functional groups (i.e., amines, thiol, nitriles, halides etc.), grafting them either by co-condensation or by post synthesis grafting procedures [12].

SBA-15 has been applied in a large variety of industrial processes after functionalization with active species on both the bulky silica framework or on the surface of the material [13–15]. These processes include: (i) oxidative transformation of hydrocarbons, such as alkanes [16,17], alkenes [18,19] and aromatic derivatives [20,21]; (ii) oxidative transformation of alcohols [22]; (iii) CO oxidation [23]; reduction processes [24] Knoevenagel reactions [25]; waste water treatments [26,27]; and carrier applications in drug-delivery [28,29].

Environmental concerns associated with novel stringent European regulations for the tolerance limits of pollutants in the atmosphere [30] highlighted the interest for the application of SBA-15 materials in the removal of sulfur-containing compounds from petroleum, a process that is indicated as "deep desulfurization" [31]. Sulfur-containing compounds, such as thiols, sulfides and disulfides, produce sulfur oxides (SO_x) upon combustion, that act as pollution agents at the global level, inducing acid rain and the formation of fine particulate matter of metal sulfates [32–34]. To avoid this problem, reductive hydrodesulfurization (HDS) is a well-stablished technology applied at the industrial level to purify crude fuel oils [35]. As a general procedure, this reaction is performed by using hydrogen in the presence of organometallic transition metal species as heterogeneous catalysts at both high temperature (up to 400 °C) and pressure (up to 100 atm) [36–38]. The application of SBA-15 in HDS processes has been reported and reviewed, encompassing the incorporation of Al^{3+}, Ti^{4+} and Zr^{4+} cations into the original material to improve the catalyst activity. In the functionalization procedure, the post-synthesis grafting was more effective than the direct synthesis method, leading to a larger pore diameter and the limited diffusion of reactants [39]. However, HDS can yield only limited desulfurization, since refractory sulfur derivatives, such as alkyl-substituted benzothio-phenes (BTs) and dibenzothiophene (DBT), are resistant to reductive treatment [40,41] due to their high alky chain steric hindrance that makes the approach to the catalyst surface difficult [42]. Moreover, the reactivity of thiophene derivatives further decreases in the presence of polyaromatics and nitrogen-containing compounds, which are often components of low quality diesel fuel compounds [43,44].

For this reason, high temperature and pressure, as well as costly hydrogen consumption, are necessary to achieve ultra-low deep desulfurization (that is, to reach a sulfur concentration lower than 10 ppm) [45]. The oxidative desulfurization (ODS) is considered the most promising technology alternative to HDS [46]. In this latter case, the recalcitrant sulfur compounds are oxidized to corresponding sulfoxides and sulfones, followed by distillation, liquid–liquid extraction, or solid–liquid adsorption removal procedures [47]. ODS is accomplished using *t*-butyl-hydroperoxide (TBHP) [48], superoxides [49], sodium bromate ($NaBrO_3$) [50] and hydrogen peroxide (H_2O_2), along with mixtures of formic acid with H_2O_2 [51–54] as primary oxidants. Hydrogen peroxide is the oxidant of choice for ODS, since it is a low cost, mild and environmentally benign reagent [55]. In this latter case, highly active transition metal derivatives have been selected for the activation of H_2O_2, often after immobilization on appropriate supports [56–59], and in alternative reaction solvents [60] [61,62]. Examples on the application of microporous and mesoporous material in ODS procedures have been previously reported [63], focusing on the application of mesoporous TiO_2 [64], titanium-containing mesoporous molecular sieves [65] and MCM-41 [66], mesoporous phosphotungstic acid/TiO_2 nanocomposites [67], mesoporous TS-1 using a hybrid SiO_2-TiO_2 xerogel procedure [68,69], vanadium polyoxometalate supported on mesoporous MCM-41[70] and phosphotungstic acid containing ionic liquid immobilized on magnetic mesoporous silica rod systems [71].

In the following sections, we will focus on the application of SBA-15 based catalysts in ODS, classifying them in terms of different families depending on the properties of the prevalent catalytic species as follows: (i) titanium oxides; (ii) vanadium oxides; (iii) molybdenum oxides; (iv) iron oxides; (v) tungsten oxides; (vi) silver oxides; (vii) polyoxometalates and (viii) miscellanea. This choice helps the reader to focus upon the role played by the metal (or metals) species in the oxidation system, highlighting the occurrence of specific synergy events with the SBA-15 support.

2. Titanium Oxides

Titanium dioxide TiO_2/SBA-15 materials have been applied as catalytic adsorptive desulfurization systems (CADS) [72], by coupling between the oxidation of recalcitrant sulfur compounds and the selective adsorption of polar products on the SBA phase [73]. As an example, a large panel of TiO_2/SBA-15 catalysts, differing in the loading of the active species, was prepared by an application of the facile wetness impregnation technology [74]. In this procedure, SBA-15 was treated with tetrabutyl titanate in ethanol under assisted ultrasound conditions [75]. Irrespective of the loading value, the titanium anatase phase largely prevailed in the samples, the active species being well dispersed on SBA-15 as a consequence of the strong electrostatic adsorption of the TiO_2 precursor on SBA-15 with a low point of zero charge [76]. The efficacy of novel TiO_2/SBA-15 was evaluated in the removal of DBT, MDBT and DMDBT as selected substrates, by comparing the simple adsorptive desulfurization capacity (ADS) [77] with the properties of the CADS approach (Figure 2). In this latter case, cumene hydroperoxide was used as the primary oxidant in acetonitrile at 35 °C. As a general trend, these CADS were two orders of magnitude more efficient than simple ADS, showing a desulfurization capacity higher than the previously reported UV-photocatalytic CDAS-TiO_2/SiO_2 procedure [78]. Under optimal experimental conditions, high desulfurization uptakes of 19.3, 12.7 and 7.2 mg-S/g-sorb were obtained. Different interaction sites were operative during these ADS and CADS processes. For CADS, TiO_2 was considered as the main adsorption site for recalcitrant sulfur compounds [79], while for ADS, the recognition site was localized in the correspondence of the silanol groups of SBA-15 [80], probably involved in the formation of hydrogen bonds [81] with sulfur oxidized products. Additionally, TiO_2/SBA-15 catalysts were used for five consecutive adsorption-regeneration cycle tests by acetone washing of the system followed with oxidative air treatment.

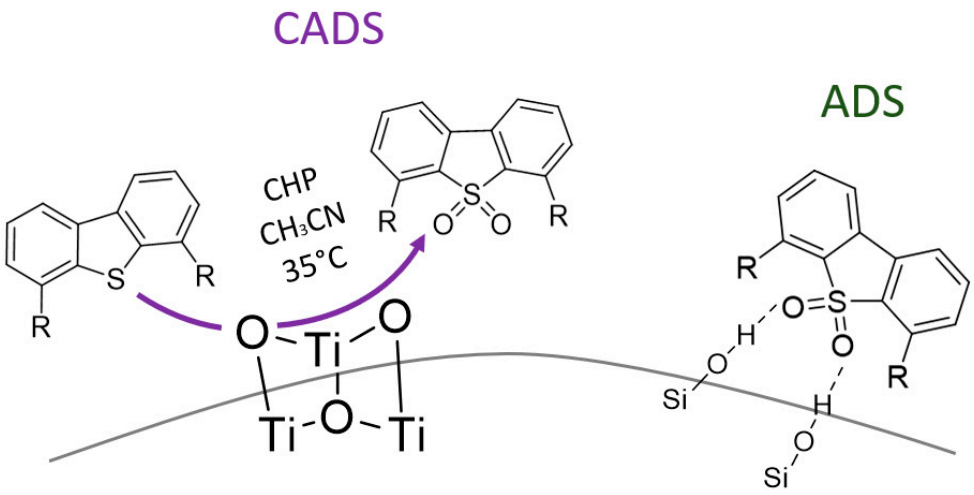

Figure 2. Schematic representation of the catalytic adsorptive desulfurization systems (CADS) versus the simple adsorptive desulfurization capacity (ADS) mechanism operating during the removal of recalcitrant sulfur compounds by TiO_2/SBA-15 catalysts.

Mesoporous Ti-silica (pore size > 2 nm) showed higher catalytic activity and longer lifetimes than its microporous counterpart (pore size < 2 nm), such as titanium silicalite TS-1, thanks to larger access to the active site and the presence of coordinatively unsaturated tetrahedral titanium able to interact with the primary oxidant [82,83]. In accordance with these data, large cylindrical mesopores Ti-SBA-15 catalysts (pore size > 7 nm) have been prepared by post-grafting insertion of titanium alkoxide/acetylacetone (acac) chelates favoring the dispersion of tetrahedral Ti^{4+} sites on the mesopore surface of the material, followed by the generation of hydrophobic surface sites by treatment with tetramethyldisilazane (TMDS) to avoid poisoning effects of the polar sulfoxide and sulfone products [84,85]. TEOS was used as the silicon source and Pluronic P123 as the structure-directing agent, working at different temperatures (35 °C, 100 °C and 140 °C) in order to control the size of the mesopores [86,87]. This procedure allows the deposition of highly dispersed Ti^{4+} sites on the surface of the parent material without any appreciable modification of the original morphology, making easy the accessibility to active species [88]. The titanium contents [Ti/Si molar (atomic) ratio] in the novel Ti-SBA-15 catalysts were included in the range between 0.7% to 4.7%, and the pore size and pore volume increased by increasing the aging temperatures [89,90]. The novel catalysts have been applied in the oxidation of benzothiophene (BT), dibenzothiophene (DBT), 4-methyldibenzo–thiophene (4-MDBT) and 4,6-dimethyldibenzothiophene (4,6-DMDBT) as representative sulfur-containing compounds present in middle distillates [91]. The reaction was performed in an *n*-heptane/toluene mixture (8:2 wt %) at 80 °C under atmospheric pressure using an excess of cumene hydroperoxide (CHP) (CHP: Sulfur compounds 2:1) as its primary oxidant, to yield the corresponding sulfone derivatives (Figure 3).

All of the novel Ti-SBA-15 catalysts showed largely superior ODS activity compared to Ti-SBA-15 prepared by the conventional impregnation method, as a consequence of the presence of the desired active tetrahedral Ti^{4+} sites. Irrespective of the nature of the sulfur-containing substrates, quantitative conversion was obtained within half an hour at 80 °C. Similar rate constants were observed in the oxidation of DBT, 4-MDBT and 4,6-DMDBT for each catalyst at a given Ti loading, suggesting that the efficacy of Ti-SBA-15 materials was independent from the actual electron density and steric hindrance of the sulfur substrates. The loading of titanium, as well as the porosity degree of the catalyst, were found to be critical parameters for the activity of the system. The novel Ti-SBA-15 catalysts were also effective in the ODS of a residue hydrodesulfurization (RHDS) diesel sample containing 200 ppmw of refractory sulfur compounds, under fixed bed reactor conditions at 80 °C. The highest reactivity was again obtained for catalysts with the largest titanium loading and pore size.

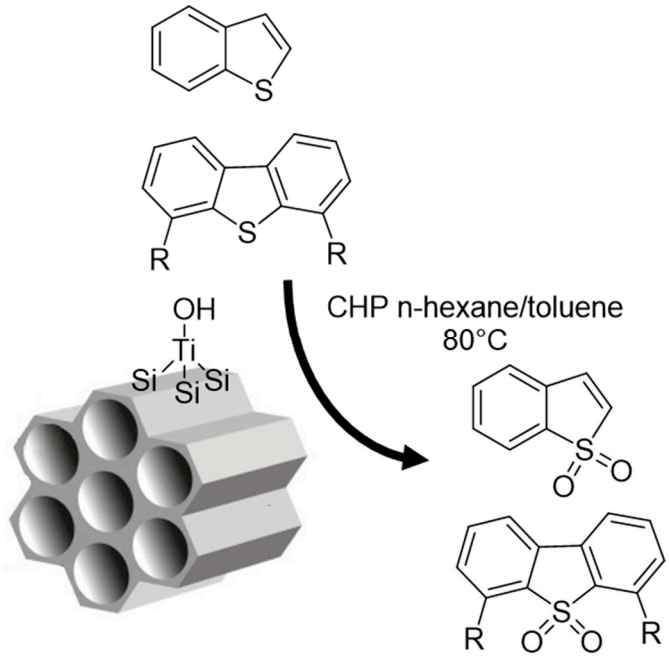

Figure 3. Schematic representation of the ODS process by active tetrahedral Ti^{4+} sites in Ti-SBA-15 catalysts.

With the aim to evaluate the effect of nitrogen compounds in the efficacy of the Ti-SBA-15 based ODS procedure, a catalyst produced by tetrabutyl orthotitanate (TBOT) grafting procedure [92] was applied for the oxidation of recalcitrant sulfur compounds in the presence of indole, carbazole and quinoline, as selected compounds commonly found in feed oils [93]. Reactions were performed by treating model sulfur and nitrogen compounds with an excess of tert-butyl hydroperoxide (TBHP) (TBHP/S-compound ratio = 2.5) for 1 h at 80 °C [94]. With respect to the simple ODS treatment, the Ti-SBA-15 activity was found to be drastically decreased in the presence of nitrogen compounds, in the following order: indole > quinoline > carbazole. These data were in accordance with results previously reported for the inhibitory effect of nitrogen compounds on MoO_3/Al_2O_3 [95] and V_2O_5 catalysts [96] in ODS processes. The mechanism of inhibition may depend on the basic or non-basic properties of the nitrogen compound, the ODS of thiophene being inhibited only by basic conditions, while that of BT being affected by both basic and non-basic nitrogen compounds [97]. Remarkably, the overall ODS activity of Ti-SBA-15 increased in the presence of aromatic and aprotic solvents, such as tetralin, 1-methylnaphthalene and acetonitrile, respectively, due to the detected high solubility of both oxidized sulfur and nitrogen compounds in these reaction media.

As an alternative, trimethylammonium-functionalized SBA-15 polyoxometalate ($(PW_{11}Ti)_2OH$@TMS-SBA-15) has been applied in ODS procedures [98]. Ti(IV) easily substitutes the W(VI) metal center in the Keggin-type POMs, creating multicenter catalytic active sites with corner- or edge-sharing TiO_6 octahedra, associated with oligomeric species by the formation of Ti–O–Ti bonds [99,100]. The preparation of the catalyst was performed through an impregnation technology specifically designed for the immobilization of polyoxometalates in SBA-15 materials [101,102], starting from freshly functionalized SBA-15 with *N*-trimethoxysilypropyl-N,N,N-trimethyl-ammonium chloride (TMS-SBA-15) and $(PW_{11}Ti)_2OH$. Under these experimental conditions a loading of 0.045 mmol/g of $(PW_{11}Ti)_2OH$ was obtained, the absence of peaks characteristic for $(PW_{11}Ti)_2OH$ in the XRD analysis strongly suggesting that the inorganic anions have been successfully incorporated inside the TMS-SBA-15 channels. The catalyst $(PW_{11}Ti)_2OH$@TMS-SBA-15 was then applied in the oxidation of a mixture of BT, DBT, 4-MDBT and 4,6-DMDBT in *n*-octane/acetonitrile (total sulfur concentration of 2350 ppm), using an excess of H_2O_2 as the primary oxidant (H_2O_2/S-compounds = 1:9) at 70 °C (Figure 4). The reaction proceeded by the transformation of the μ-hydroxo dimeric $(PW_{11}Ti)_2OH$

into the active peroxo compound $[HPW_{11}O_{39}TiO_2]^{4-}$ [103]. After 2 h, complete desulfurization was achieved. The lower activity observed for $(PW_{11}Ti)_2OH$@TMS-SBA-15 with respect to the homogeneous counterpart $(PW_{11}Ti)_2OH$ was probably due to the presence of kinetic barriers for the access of substrate at the heterogeneous active site. The oxidative reactivity order DBT > 4-MDBT ≥ 4,6-DMDBT > BT was in accordance with electronic density effect and with some steric hindrance [104,105]. Moreover, $(PW_{11}Ti)_2OH$@TM-SBA-15 retained its structure and morphology after five consecutive ODS cycles.

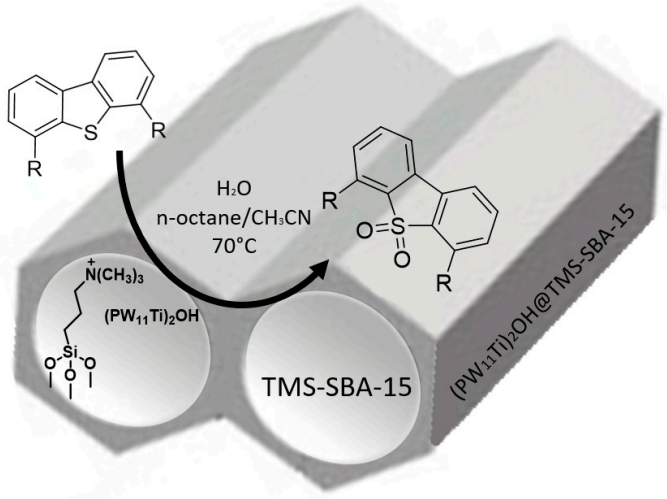

Figure 4. Oxidation of sulfur-containing compounds by the $(PW_{11}Ti)_2OH$@TMS-SBA-15/H_2O_2 system.

3. Vanadium Oxides

The use of vanadosilicates in ODS/ H_2O_2 processes has been reported to achieve a desulfurization yield higher than 80% [106]. In these reactions, mesoporous vanadosilicates showed higher activity than materials having different pore-size distribution, confirming the beneficial role of large-surface-area, wider pore size and thicker pore walls on the interaction between the active site and the substrate [107,108]. On the basis of these results, vanadium oxide (V_2O_5) was incorporated into the SBA-15 framework by a controlled grafting process, affording highly dispersed vanadium sites with distorted tetrahedral VO_4 units on the silica surface [109]. These catalysts showed significative CODS activity when compared with other V_2O_5 supports (alumina, titania, ceria and niobia); the highest activity being obtained in the presence of tetravalent cations [110]. As an improvement of this study, vanadium oxide species were incorporated into SBA-15, and modified aluminum Al-SBA-15 and gallium Ga-SBA-15 materials, by both direct-synthesis and impregnation methodology [111].

In the first case, VCl_3 was added to the pluronic 123/TEOS mixture (V/Si ratio of 1/30 and 1/54) to yield V-SBA-15, while in the second case, VO_x-SBA-15, VO_x-Al-SBA-15 and VO_x-Ga-SBA-15 were obtained by treating the appropriate SBA-15 starting material with an aqueous solution of VCl_3 followed by calcination at 500 °C. As a general trend, the incorporation of Al and Ga improved the dispersion of vanadium species, probably due to a better anchorage of the active species on more acidic supports. Irrespective from the applied procedure, the small angle X-ray diffraction analysis (XRD) showed that SBA-15 retained its mesoporous structure after the incorporation of aluminum and gallium [112], with small clusters of vanadium oxide species being highly dispersed on the surface of the support. However, N_2 adsorption–desorption isotherm analysis showed a partial loss of the structure of the catalysts from the impregnation method in the correspondence of the highest value of vanadium loading, as a consequence of the incorporation of vanadium species into the mesoporous channels. In contrast, pore diameter had a marked increase when vanadium was introduced by direct synthesis, suggesting that vanadium atoms in part replaced Si atoms [113]. VO_x-SBA-15 efficiently converted DBT to corresponding sulfone in acetonitrile using H_2O_2 as a primary oxidant, the highest conversion (100%) being obtained with the ratio V/Si = 1/30, corresponding to the prevalence of

pseudo-tetrahedral VO_4^{3-} species on the surface of the catalyst. Samples characterized by the higher loading value of vanadium showed lower activity as a consequence of the formation of less active VO_x microcrystal chains. The modification of SBA-15 with Al and Ga further increased the desulfuration activity of VO_x-Al-SBA-15 and VO_x-Ga-SBA-15 catalysts, probably due to the formation of a larger number of highly dispersed VO_4^{3-} species, associated with synergic effect of Lewis and Bronsted acid sites, derived from Ga or Al incorporation [114]. On the other hand, lower activity was found when vanadium was incorporated via direct synthesis in V-SBA-15, due to the presence of a kinetic barrier for the interaction between the active sites and DBT. The experimental design optimization of the ODS of DBT using the VO_x-Ga-SBA-15 prepared by the impregnation method from $Ga(NO_3)_3$ has been more recently reported [115]. The higher levels of the oxidation of DBT were obtained employing the catalyst with 4 wt % of gallium and 6 wt % of vanadium, the optimal ratio in weight between DBT and VO_x-Ga-SBA-15 being 4 at the H_2O_2/DBT molar ratio value of 5.

Examples of the application of VO_x-SBA-15, prepared by the impregnation method from ammonium metavanadate (NH_4VO_3) and SBA-15, using molecular oxygen (O_2) as oxidant and the ionic liquid 1-butyl-3-methylimidazolium tetrafluoroborate [Bmim]BF_4 as a selective extraction phase, are reported [116]. In this catalytic system, the recalcitrant sulfur compounds (DBT, 4-MDTB and 4,6-DMDTB) are firstly extracted from the oil phase to the ionic liquid in which the VO_x-SBA-15 catalyst is suspended. After the extraction step, the oxidation proceeds by vanadium activation of ionic liquid adsorbed molecular oxygen (O_2) with formation of the corresponding radical anion derivative and successive oxygen atom transfer to sulfur [117]. The sulfones produced during the oxidation are successively removed from the surface of the catalyst thanks to the high solubility property of the ionic liquid, thus reducing the inhibitory effect that these products normally exert after their adsorption on SBA-15 (Figure 5) [118]. Under the optimal experimental conditions, the removal of DBT, as one of the most stable residues in the hydro-desulfurization (HDS) process, reached up to 99.3% (<3.5 ppm) after 7 h at 120 °C.

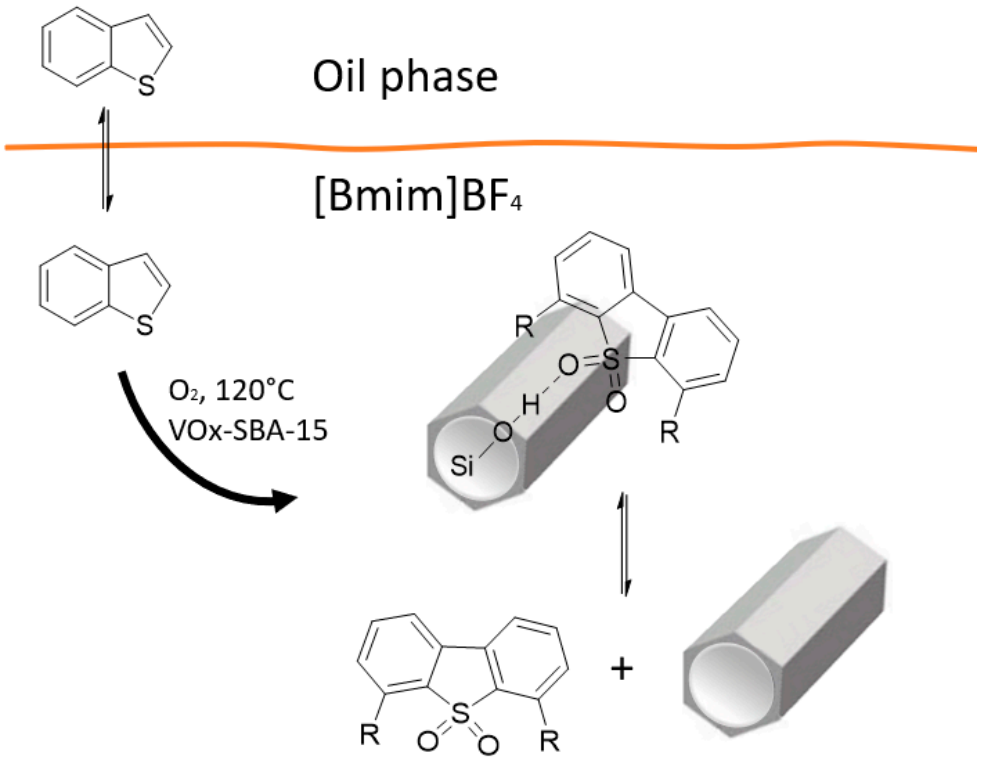

Figure 5. The extractive-catalytic desulfurization oxidative cycle of VO_x-SBA-15 in the presence of 1-butyl-3-methylimidazolium tetrafluoroborate.

4. Molybdenum Oxides

The use of high oxidation states molybdenum Mo(VI) derivatives in the ODS procedure has been reported [119]. For example, MoO_3 supported on amorphous silica afforded 82% reduction of the residual sulfur compounds in pre-hydrotreated diesel samples after activation with cumene hydroperoxide at 70 °C [120]. The activity of MoO_3/SiO_2 further increased after the introduction of different alkaline earth metals (Ca, Ba, Sr and Mg) in the silica phase [121], highlighting the key role played by the Lewis and Bronsted acid sites in the behavior of the oxidation [122]. In order to prepare molybdenum ODS catalysts with larger surface area and larger pore diameter, CoMo/SBA-15 compounds were obtained by impregnating the SBA-15 phase with alcoholic solutions at different concentrations of $Co(NO_3)_2{\cdot}6H_2O$ and $(NH_4)_6Mo_7O_{24}{\cdot}4H_2O$, respectively [123]. The XRD analysis confirmed the retention of the mesoporous structure after the impregnation procedure with a slight alteration of the loop shape and pore distribution with respect to original SBA-15, due to percolation of Co and Mo oxides within mesopores, associated with a high dispersion of the metal oxides on the surface of the catalyst. Only Lewis acid sites were found on the surface of the novel catalysts, corresponding to a mixture of different molybdenum species. In particular, the structural analyses showed that the amount of MoO_3 microcrystals increased with respect to the β-$CoMoMoO_4$ phase by increasing the overall CoMo concentration [124,125]. CoMo/SBA-15 catalysts were studied in the oxidation of DBT in *n*-hexadecane, using H_2O_2 as a primary oxidant under a large panel of reaction temperature (from 60 °C to 80 °C) for 1h at atmospheric pressure. Irrespective of the loading of the catalyst, the activity decreased at higher temperature as a consequence of both H_2O_2 decomposition and lowering of the amount of the Lewis acid sites. In the optimal catalyst condition (that is, 20% in weight of (Co+Mo) metal oxide loading), a 90% conversion value of DBT was obtained at 60 °C. As evidenced by Raman spectra, the cobalt modified molybdate MoO_3 microcrystals were the main active species during the oxidation of DBT, while β-$CoMoO_4$ substantially inhibited the oxidative process.

The role that the defective structure of dispersed MoO_3 active sites can play in the ODS procedure was successively evaluated by a deep analysis of the oxidation behavior of 4,6-DMDBT with the MoO_3/SBA-15 catalyst [126]. MoO_3/SBA-15 was prepared via impregnation of SBA-15 with different amounts of ammonium heptamolybdate (from 5 wt/% to 25 wt/%) as molybdenum precursor. The integrity of the mesoporous structure was found to be dependent from the loading factor, the regular mesoporous feature being observed within to 15 wt/% of Mo, after which the collapse of the structure gradually occurred [127]. XRD analysis of catalysts with 5, 10 and 15 wt/% of MoO_3 showed the presence of highly dispersed molybdenum species with an average size smaller than 4 nm. At a higher loading value, orthorombic α-MoO_3 crystals, with a certain oxygen deficiency, were formed [128]; the crystallite size being increased by increasing the amount of molybdenum. The oxygen defects are electron-deficient Lewis acid sites and may serve as surface active centers for surface adsorption and reaction. The presence of α-MoO_3 crystals in 20 and 25 wt % MoO_3/SBA-15 catalysts was further confirmed by Raman and XPS analyses [129]. The novel MoO_3/SBA-15 catalysts were evaluated in the oxidation of 4,6-DMDBT with H_2O_2 in *n*-hexadecane at different reaction temperatures (from 50 °C to 70 °C) for 1 h, in the presence or in the absence of formic acid as co-oxidant species. Performic acid (HC(O)OOH) is easily produced by reaction between H_2O_2 and formic acid [130]. As a general trend, the conversion of 4,6-DMDBT was found to be proportional to the number of Lewis acid sites present on the surface of the catalyst during the oxidation performed with H_2O_2 alone, the highest conversion value being obtained in the correspondence of the higher loading factor (15–20 wt/%). In the presence of formic acid, 4,6–DMDBT oxidation was significantly affected by the formation of surface peroxometallic complex and Lewis acidity. Under the optimal reaction condition using 15 and 20 wt % MoO_3/SBA-15 catalysts and the H_2O_2/formic acid mixture, more than 99% 4,6–DMDBT could be removed at 70 °C within 30 min. Figure 6 describes the suggested mechanism for the oxidation performed with the H_2O_2/formic acid mixture. In this reaction, scheme performic acid is coordinated by Mo^{6+} ions to generate a reactive peroxometallic complex [131] able to transfer the oxygen atom to the substrate. In this process, oxygen defective α-MoO_3 sites can perform as molecular

recognition sites for 4,6-DMDBT. As suggested by the authors, when the amount of MoO_3 was greater than 20 wt % (i.e., 25 wt % MoO_3), the presence of the largest MoO_3 particles lead to lower dispersion and a lower number of exposed Mo ions, thus disfavoring the 4,6-DMDBT adsorption and oxidation.

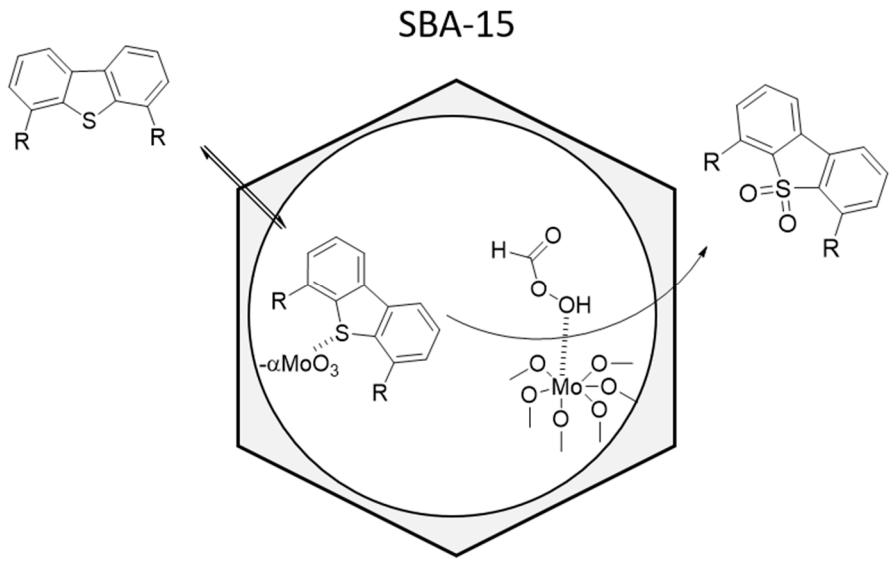

Figure 6. Schematic representation of the oxidation of 4,6-DMDBT with MoO_3/SBA-15 using the H_2O_2/formic acid mixture. Reactive Mo peroxometallic complex transfers the oxygen atom to the substrate, while oxygen defective α-MoO_3 sites perform as specific molecular recognition sites.

5. Iron Oxides

Iron-based ionic liquids with redox properties have been applied in ODS processes, thanks to their high reactivity and capability to extract polar sulfone and sulfoxide derivatives from the crude oil [132]. Examples of desulfuration processes mediated by iron-based ionic liquids are reported, including the use of 1-*n*-butyl-3-methylimidazolium metal chloride derivatives [C_4mim] Cl/MCl_2 (M = Zn, Fe, Cu, Mg, Sn, Co) [133], dialkylpyridinium tetrachloroferrates ionic liquids [C_4MPy] $FeCl_4$ [134] and Fenton-like ionic liquids [135,136]. The activity and recyclability of iron-based ionic liquids was significantly improved by the immobilization of appropriate precursors on SBA-15, as in the case of the preparation of 1-methyl-3-(trimethoxysilylpropyl)-imidazolium [pmim] tetrachloro-ferrate/SBA-15 catalyst, namely [pmim]$FeCl_4$-SBA-15. The synthetic procedure for the synthesis of [pmim]$FeCl_4$-SBA-15 required two successive steps (Figure 7): (i) the grafting of [pmim]Cl on SBA-15 to yield the [pmim]Cl-SBA-15 intermediate and (ii) the ion exchange of chorine with tetrachloroferrate by treatment of [pmim]Cl-SBA-15 with $FeCl_3$ in acetonitrile [137].

The XRD analysis of [pmim] $FeCl_4$-SBA-15 showed a long-range, ordered structure with a well-defined hexagonal lattice (p6mm) motif, associated with the expected functionalization of the mesopore channels, as highlighted by the expected decrease in the intensity of the peaks [138]. The textural properties of SBA-15 were substantially maintained after immobilization of [pmim] Cl and on subsequent anchoring of $FeCl_4^-$. The [pmim] $FeCl_4$-SBA-15 was applied in the ODS of a model fuel sample obtained by dissolving DBT, BT and DT in *n*-octane, using H_2O_2 as the primary oxidant. The concentration of sulfur compounds in the model fuel decreased in the order of DBT > BT > DT, with an overall 94.3% removal of DBT in the optimal conditions, consisting in the presence of [Omim] BF_4 as a co-solvent. As suggested by the authors, the reaction proceeded with the initial extraction of sulfur compounds from the oil, followed by a Fenton-like oxidation process.

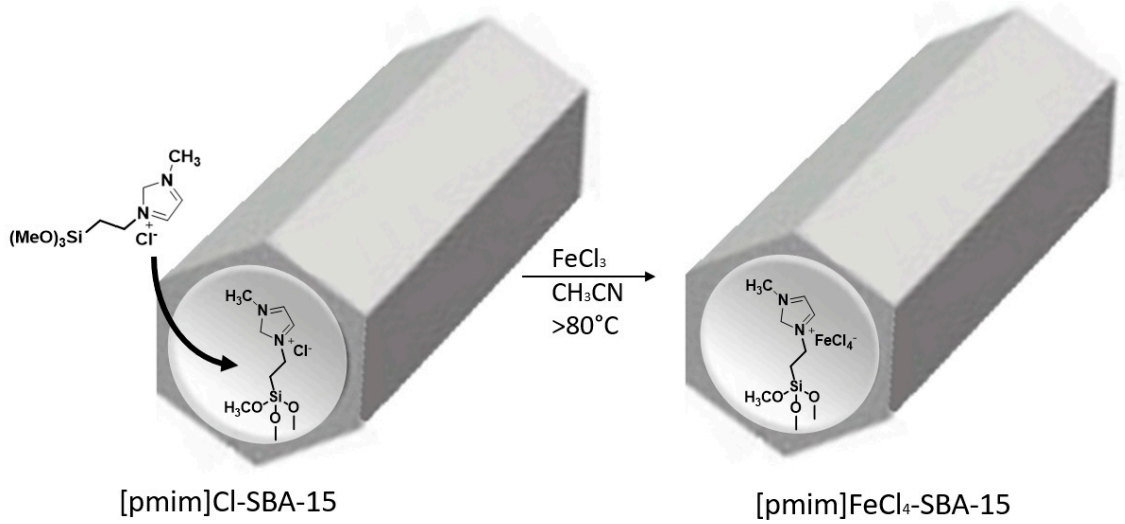

Figure 7. Preparation of iron-based redox ionic liquid [pmim] $FeCl_4$ supported on SBA-15.

As an alternative, the Fe-SBA-15 catalyst was prepared by an impregnation procedure, using $Fe(NO_3)_3 \cdot 9H_2O$ as source of iron [139]. Fe-SBA-15 showed well-resolved XRD diffraction peaks, confirming the p6mm hexagonal symmetry of mesostructured SBA-15. The decrease of the peaks' intensity suggested a slight distortion in the material, with a partial diminution of the pore's diameter, due to the lower ionic radio of Fe with respect to Si [140–142]. In particular, Fe-SBA-15 contained a well-dispersed hematite phase (α-Fe_2O_3) without any presence of the magnetite phase (Fe_3O_4).

To evaluate the ODS capacity, Fe-SBA-15 was applied in the oxidation of BT, DBT and 4,6-DMDBT, in a three-phase system (*n*-dodecane, acetonitrile and catalyst), with H_2O_2 as primary oxidant at 60 °C. Under these experimental conditions, more than 90% of sulfur was removed in the first 15 min of reaction time, DBT showing the higher reactivity as a consequence of its recognized high electron density on the sulfur atom [143]. Note that Fe-SBA-15 was less reactive than Fe-MCM-48 under similar experimental conditions, probably due to the difference in surface area, pore volume and dispersion of the active sites. Ultrasound-assisted technology improved the efficacy of iron-based SBA-15 catalysts. For example, Fe-SBA-15 and Fe/Zr-SBA-15 catalysts with high ODS capacity have been prepared from the corresponding mineral supports by an ultrasound-assisted procedure, using $Fe(NO_3)_3 \cdot 9H_2O$ as the iron source [144]. Irrespective of experimental conditions, spectroscopic data indicated the presence of a well dispersed hematite phase (in both α-Fe_2O_3 and γ-Fe_2O_3 forms) as an active species. Both catalysts showed the presence of Lewis acid sites, which amount increased by increasing the iron loading. The catalytic activity of Fe-SBA-15 and Fe/Zr-SBA-15 was evaluated in the oxidation of DBT in *n*-hexadecane and H_2O_2 as the primary oxidant. As a general trend, the higher activity was observed in the presence of the highest value of loading of Fe (30 wt/%), Fe/Zr-SBA-15 being more active than Fe-SBA-15, probably as a consequence of the role played by the zirconium-increased surface acidity in the promotion of γ-Fe_2O_3 with respect to the formation of amorphous, and less reactive, iron oxide.

6. Tungsten Oxides

Nitrogen functionalized active materials have been successfully applied in heterogeneous catalysis [145,146], including the oxidative transformations of sulfur derivatives [147–149], thanks to the high coordinative capability of the nitrogen-containing framework towards metal species [150,151], associated with tunable acid-base properties. With the aim of obtaining a solid catalyst, to be employed in the ODS of gasoline, with large specific surface and high catalytic activity, WO_3 was introduced, for the first time, into the SBA-15 mesoporous molecular sieve, under conventional hydrothermal conditions in strong acidic solution, using H_2WO_4 as a tungsten source in the presence of P123 triblock copolymer and cetyltrimethylammonium bromide as template. This system showed a promising oxidation activity, being able to reduce the sulfur content of gasoline (540 ppm) up to 91% in 80 min [152]. Examples of

the preparation and application of tungstate nitrogen-containing catalysts are reported [153], nitride derivative being used in the oxidation of model sulfur compounds under visible light [154]. With the aim of further improving green applications of tungstate nitrogen-containing catalysts, WOx/N-SBA-15 materials have been prepared and used in the ODS procedure [155]. WOx-SBA-15 was prepared as starting material by direct synthesis in the presence of TEOS as the silica source and P123 as our structure-directing agent, using $NaWO_4 \cdot 2H_2O$ as tungstate source. Nitrogen rich WOx/N-SBA-15 was successively obtained by treating WOx-SBA-15 with a mixture of ethylene diamine $NH_2C_2H_4NH_2/CCl_4$ at reflux, followed by calcination at high temperature (600 and 800 °C). The novel catalyst showed the presence of well-dispersed WOx species in a nanocluster form, and was characterized by a channel-like pore arrangement of the 2D hexagonal (honey comb) type. The presence of nitrogen-containing CNx-like frameworks was confirmed by both Raman and X-ray photoelectron (XP) spectra, in association with graphite-like carbon originated by the ethylene diamine degradation. The CNx framework was characterized by the presence of pyridine-nitrogen-like atoms (N-py), nitrile moieties and a C–N–C graphitic-like ring motif, suggesting a complex rearrangement of nitrogen and carbon atoms during the preparation of the catalyst. WOx/N-SBA-15 was a catalyst more efficient than WOx-SBA-15 in the ODS procedure, suggesting a beneficial role of the CNx framework in the oxidation. Under optimal experimental conditions, the quantitative conversion of DBT was obtained with WOx/N-SBA-15 after 2 h at 100 °C, using H_2O_2 as primary the oxidant in acetonitrile. Moreover, the activity of the catalyst increased with the increase of the loading of the WOx species. Most probably, the reaction proceeded by the formation of highly reactive tungstate-peroxo complexes [156], even if the authors have not investigated the possible role of the CNx framework in this process.

7. Silver Oxides

Different supported silver adsorbents have been reported in the selective removal of sulfur compounds from fuels via a strong complexation mechanism, including Ag_2O/titania materials in jet fuel desulfurization [157,158], Ag^+/SBA-15 and Ag^+/SiO_2 for the selective adsorption of dibenzothiophene (DBT) [159], and Ag^+ supported zeolite and activated carbon for the adsorption of both BT and DBT [160,161]. Moreover, supported silver oxides or silver can also act as oxidative catalysts in the epoxidation of alkenes [162–164], aldehydes [165], and various organic compounds [166] and carbon oxide [167]. The capability of silver oxides to contemporarily perform as active catalytic species and adsorption phases has been applied in the ODS procedure by preparation of novel Ag_xO-SBA-15 materials and their use in the adsorption/oxidation of BT, DBT, 4-MDBT and 4,6-DMDBT, as model fuel compounds [168]. Ag_xO-SBA-15 catalysts were prepared by an ultrasound-assisted impregnation process of SBA-15 and $AgNO_3$ water solutions at different concentration. Irrespective from the loading factor, the catalysts retained the original mesoporosity of SBA-15 showing Ag_xO species uniformly dispersed in the hexagonally-ordered network (average diameter value of the particle around 5–6 nm), the presence of larger Ag_xO particles being detected only at the highest loading factor (25 wt/%). In the XRD analysis, AgO particles largely prevailed in the fresh sample, while Ag_2O and Ag become the main silver species in the aged sample, as a consequence of degradation processes occurring during the time for unstable high valence AgO oxide at the nano-size scale [169,170]. Ag_xO-SBA-15-aged samples showed a high desulfurization activity in the presence of air under ambient conditions. The addition of air dramatically enhanced the activity with respect to the simple adsorption processes. On the other hand, freshly prepared Ag_xO-SBA-15 catalysts showed a remarkable desulfurization capacity even in the absence of air. In this latter case the desulfurization capacity followed the order of 4,6-DMDBT > 4-MDBT > DBT > BT, consistent with the order of sulfur electron density on the substrate. Irrespective of the origin of the catalysts, sulfones were detected as reaction products in the presence of air. Noteworthy, sulfones were also detected with freshly prepared Ag_xO-SBA-15 catalyst in the absence of air, suggesting that this catalyst may also perform as an endogenous source of oxygen for the oxidation. The general reaction mechanism for fresh and aged Ag_xO-SBA-15 catalysts is described in Figure 8.

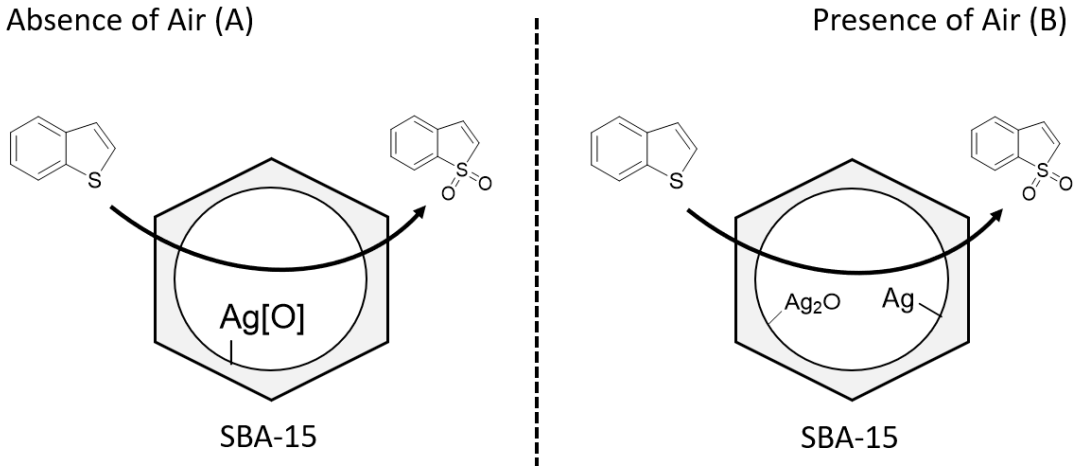

Figure 8. Schematic representation of the oxidation of sulfur compounds in the presence of Ag_xO-SBA-15. Panel **A**: Freshly prepared catalysts in the absence of air. Panel **B**: Aged catalyst in the presence of air.

Surface-distributed, nano-size [O]-retaining AgO active sites are responsible for the oxygen atom transfer from freshly prepared Ag_xO-SBA-15 catalyst to substrate in the absence of air (Panel A). A different mechanism occurs with aged Ag_xO-SBA-15 in the presence of air (Panel B), in which case Ag_2O and metallic Ag become the main active species for the direct activation of dioxygen [171]. During the aging AgO is progressively transformed into Ag_2O.

8. Polyoxometalates

Polyoxometalates (POMs) are formed by cations and polyanion clusters having structural diversity (Figure 9), where the basic construction units are based upon the MO_x (x = 5, 6) oxometal polyhedral [172–174]. The M species are early transition metals (e.g., V, Nb, Ta, Mo, W, and so on) at their highest oxidation states. Some polyanions are centered by heteroatoms (X) that significantly affect their properties. These heteroatoms are usually main-group elements, including Si, P, S, Ge, As, Se, B, Al and Ga, but are not limited to these. The bulky polyanions have a highly negative charge, and their surfaces are rich of oxygen atoms able to donate electrons; consequently, they can be considered as soft bases. At the same time, the metal ions on the skeleton of polyanions possess unoccupied orbitals, able to accept electrons. By this way, polyanions can also act as Lewis acids. Hence, POMs may play the roles of Lewis acid and Lewis base, under different conditions. Generally speaking, the protonation of an oxometallate ion under particular conditions (e.g., pH, concentration, temperature, solvent) gives rise to the polycondensation of the tetrahedral MO_4^{2-} units and the formation of more complex structures called polyanions:

$$nMO_4^{2-} + 2mH^+ \rightleftharpoons M_nO_{(4n-m)}^{(2n-m)-} + mH_2O$$

If the condensation occurs between similar species, the reaction yields an octahedral isopolyanion (IPA) having the general formula $M_nO_{(4n-m)}^{(2n-m)-}$ (usually n 6). Conversely, if the condensation of the oxoanions occurs around either, a central heteroatom (e.g., X = Si, P, As, Ge, etc.) or another metal atom, the reaction leads to the formation of a heteropolyanion (HPA) with the general formula of $X_sM_nO_m^{y-}$. Depending on experimental assembling conditions, POMs are formed by IPAs and HPAs, having two main structures, namely (i) *Keggin* (X/M = 1/12) and (ii) *Dawson* (X/M = 2/18) type structures. The many different elements which can act as heteroatoms in HPA complexes with various coordination numbers leads to the formation of several other complex polyhedra structures known as Anderson, Lindqvist, Waugh and Silverton (Figure 9) [175].

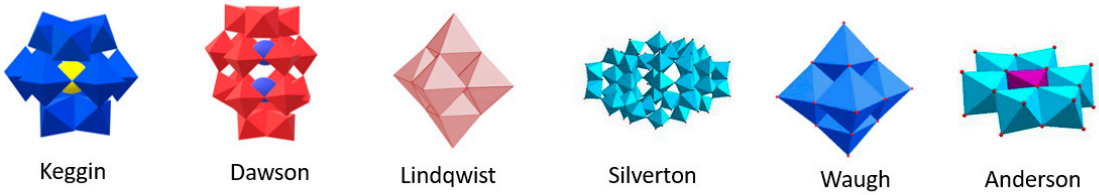

Figure 9. Sketches of classical polyoxometalates (POMs) structures in polyhedral illustrations.

The Keggin type HPAs containing tungsten or molybdenum addenda atoms have received great attention for the very variable chemical properties, which may be easily tuned through changes in their composition and structure. The replacement of their protons by large radium cations (i.e., Cs^+) makes insoluble the Keggin HPAs and increases their surface area and thermal stability [176]. On the other hand, the removal of tungsten or molybdenum atoms from the parent structure generates vacancies (Lacunar Keggin HPA), which can give them alternative catalytic activity [177].

In spite of an overgrowing interest toward the preparation of a huge number of inorganic–organic hybrid architectures based on POMs, due to their extreme versatility of compositions, high structural stability and special properties like strong acidity and rich redox chemistry, at the same time these compounds frequently show several drawbacks. They have, indeed, relatively small specific surface areas that hinder accessibility to their active sites, thus reducing their catalytic activity; in addition, their high solubility in polar solvents prevents their simple recovery from complex mixtures. To avoid such disadvantages and to meet the requirement of sustainable chemistry, great effort has been focused on immobilization of the active POMs on different solid supports, such as silica with high-surface areas, activated carbon, molecular sieves and graphene or graphene oxide, to improve their dispersion and heterogeneity [178–180]. For all the above reasons, it is reasonable that the POMs compounds have received considerable interest for what concerns their use for demanding catalytic ODS processes [181], and in particular, as immobilized catalysts on mesoporous SBA-15 materials.

Hereafter, the main results obtained in the last years in the oxidative desulfurization of authentic or model fuels promoted by heterogeneous catalysts based on POMs derivatives, will be reviewed grouping the results into two main sub-categories formed, respectively, by phosphomolybdic or phosphotungstic containing POMs.

8.1. Phosphomolybdic Containing POMs

Starting about fifteen years ago, a novel phosphomolybdic (HPMo)/SiO_2 mesoporous composite was prepared by the sol–gel method, working with 12-phosphomolybdic acid, TEOS and the triblock copolymer $EO_{20}PO_{70}EO_{20}$ (Pluronic P123) as a template [182]. Authors declared that in this compound, the HPMo was highly dispersed inside the silica framework, while maintaining its original Keggin structure. The heterogeneous catalytic system was active and stable toward the ODS of a model fuel only formed by DBT, with H_2O_2 as oxidant in a large excess (O/S molar ratio = 12). Some of the same authors published another paper where the phosphomolybdic (HPMo) and phosphotungstic (HPW) heteropolyacids, were chemically anchored onto the amino functionalized SBA-15 channels, with the aim to study their catalytic activity for the ODS of model fuels [183]. The SBA-15 functionalization with aminosilane groups, through aminopropyltriethoxysilane (APTES) [184], is aimed to increase the electrostatic interactions between the amino moiety of the support and the heteropolyacid groups, thus increasing the chemical stability of the heterogeneous catalyst. Interestingly, by comparing the two catalytic systems, it was evident that the catalyst HPW/H_2N-SBA-15 was slightly more active in comparison with HPMo/H_2N-SBA-15, justifying these experimental data with the conversion of the original Keggin structure of starting HPA (with its original redox potential) into a new polyoxoperoxo species, after the oxidation with H_2O_2. On the other hand, it is known that the ability of tungsten atoms to combine with TBHP is higher than molybdenum atoms. Thus with increasing the tungsten

loading, the ability of HPAs to produce more active peroxometalate intermediates becomes stronger, also in the presence of TBHP as main oxidant.

An interesting method for the deep desulfurization of model fuels and exploitable as an alternative to severe HDS, indicated that the condensation reaction with formaldehyde catalyzed by phosphomolybdic acid inside selected supports such as SBA-15, acting both as support and adsorbent of the reaction products, was effective for the specific removal of thiophenic and benzothiophenic compounds, while preserving the fuel quality [185]. Indeed, as assessed by authors, the phosphomolybdic acid promoting the condensation reaction with formaldehyde, affording polymerization products, can occur only with thiophenic or benzothiophenic compounds, thus preserving olefins or the other aromatic components of fuels. The coupling with an oxidant as peracetic acid allowed a strong reduction in the total sulfur content lower than 15 ppm.

Frequently, the phosphomolybdic-based HPA has been modified with the addition of other metals in order to tune the catalytic activity of the corresponding POMs, according to specific requirements. This is the case of an heterogeneous catalyst based on a molybdovanadophosphoric acid framework supported on both pure SBA-15 or H_2N-SBA-15, after the silica functionalization with APTES [186].

It was observed that, in spite of a comparable high activity in the oxidation of sulfur compounds of a model oil (DBT in *n*-hexane), the catalyst $PMoV_2$/SBA-15-NH_2 formed through grafting of molybdovanadophosphoric acid onto H_2N-SBA-15, showed good recyclability in comparison of the catalyst $PMoV_2$/SBA-15 impregnated on unmodified SBA-15 silica. The higher stability against leaching of the grafted catalyst, has been attributed to the strong electrostatic binding between cation and anion due to the in situ formation of the salt ≡ $Si(CH_2)NH_3{\cdot}PMoV_2$, not possible in the unmodified silica, where only weak interactions between silanol groups and high soluble $PMoV_2$ moiety, can occur. In another case, the stability of immobilized molybdovanadophosphoric acid was increased by using zirconium modified mesoporous SBA-15 able to form insoluble salts of HPAs on the silica surface. The 11-Molybdo-vanadophosphoric acid supported on Zr-modified silica (MoV/Zr/SBA-15) worked as an active and stable catalyst for the TBHP promoted ODS of model oil [187]. It is known that, in particular cases, the length and pore size of mesoporous silica channels imply both crucial factors and effectiveness in fluid phase reactions [188]. As a consequence, channels with the larger pore size and shorter length can overcome limitations like mass transfer, accessibility and diffusion in the liquid phase reactions. For this reason platelet SBA-15, characterized by shorter channels parallel to its thickness, has been considered more promising to serve as a support for catalytic systems. Accordingly, cesium salts of tungsten-substituted molybdophosphoric acid, Cs_xH_{3-x} [$PMo_{12-y}W_yO_{40}$], (x = 1–3, y = 2–10), supported on platelet SBA-15 have been synthesized, via a two-step impregnation method, and used as oxidative desulfurization catalysts, using TBHP as oxidant [189]. It is interesting to note that for the selected $H_3PMo_8W_4O_{40}$ HPA, loaded with different amounts of cesium ion, the observed initial catalytic performances followed the order $Cs_2Mo_8W_4$/SBA > $Cs_1Mo_8W_4$/SBA > $Cs_3Mo_8W_4$/SBA. As known, HPA supported on mesoporous silica shows strong Bronsted acidity (higher Bronsted acid sites *vs* Lewis acid sites), being the Lewis acidity increased by replacing of H^+ with Cs^+ cations. It has been clarified [190] that both kinds of acid sites may be present in $Cs_1Mo_8W_4$/SBA and $Cs_2Mo_8W_4$/SBA species, even if the number of Lewis acid sites of the former catalyst is lower than that of the latter, and being the Bronsted acidity irrelevant for $Cs_3Mo_8W_4$/SBA, due to the absence of H^+ ions. As well accepted, the oxidation of sulfur substrates activated by molybdenum- or tungsten-polyoxometalate catalyst implies the formation of active peroxo species at the metal site, followed by transferring the oxygen atom to the sulfur acceptor (Figure 10).

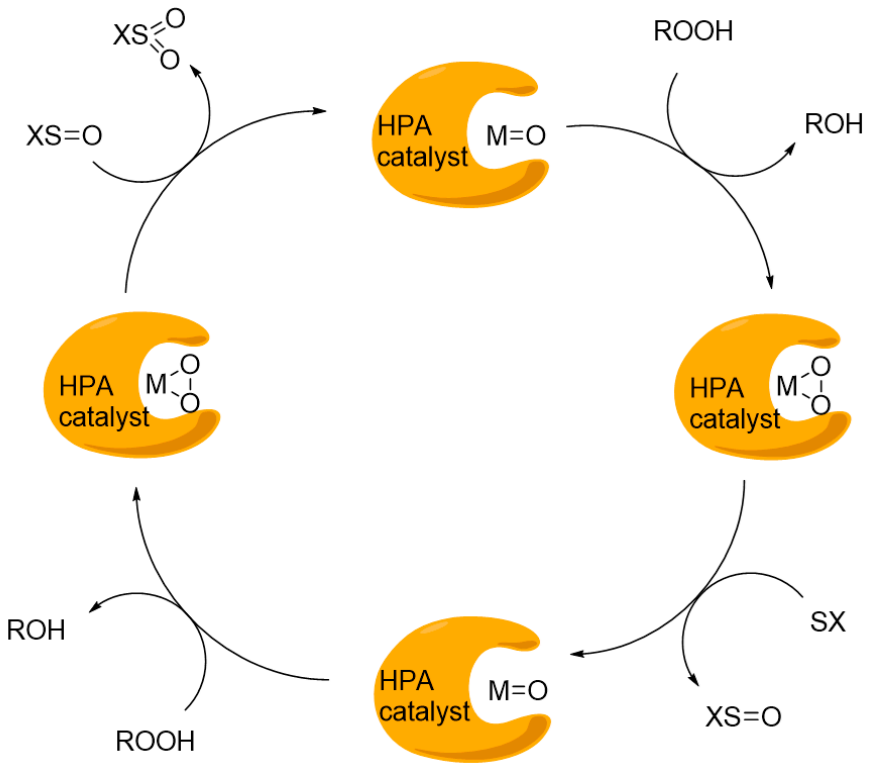

Figure 10. Proposed mechanism for the oxidation of organosulfur compounds by ROOH as oxidant and heterogeneous HPA as catalyst.

From literature, it is known that the formation of peroxo-metallate species, is energetically favored by the combined presence of Lewis and Bronsted acid sites [191]. As a consequence, it has been supposed that the presence of both Lewis and Bronsted sites on the $Cs_2Mo_8W_4$/SBA catalyst, facilitates the formation of peroxo-HPA intermediates, thus increasing the oxidation reaction efficiency.

Among several advantages on the use of mesoporous SBA-15 as versatile support for heterogeneous catalysis, one of the main drawbacks may be found on its hydrophilic nature which could be a detrimental aspect if we are dealing with the catalysis of reactions containing both aqueous phase and hydrophobic starting materials, as in the case of ODS of authentic fuels. In some cases, it has been reported that the hydrophobization of mesoporous supports could markedly enhance the stability and performance of the catalyst system. To achieve this goal, the most explored approach was based on the functionalization of SBA-15 with imidazole-based ionic liquids (ILs). Noteworthy, due to the introduction of IL, the heterogeneous catalyst exhibited good wettability for the model oil, which could provide easier access to catalytically active sites, for reagents. As a well explored general method, the doping of SBA-15 by IL was based firstly on the preparation of the appropriate precursor 1-Methyl-3-(triethoxysilylpropyl)-imidazolium chloride ([pmim]Cl) ionic liquid, by using *N*-methyl imidazolium and 3-chloropropyltriethoxysilan, and then by grafting the latter IL on SBA-15, under usual conditions. At this point, several different HPAs may be immobilized affording several different types of hybrid functional materials (Figure 11) depending on the nature of metals (M, M') and heteroatoms (X).

By this way, several authors published the preparation of heterogeneous PMOs catalysts, ranging from $HPMoV_2$ [192], to HPMo [193] based materials, all following the same immobilization procedure over the functionalized IL-SBA-15 silica. These hybrid catalysts displayed high catalytic performances for removing sulfur compounds from model oil (especially in the case of HPMo system, where the H_2O_2 oxidant was used in the lowest amount) and high stability and recyclability properties, acting both as a catalyst and as an adsorbent toward the sulfur oxidized products. Interestingly, XRD analyses confirmed that the ordered structure of SBA-15 is maintained after the IL grafting and the successive

HPA loading. Concerning the latter point, an optimal value should be carefully chosen in order to avoid that IL-SBA-15 channels can be blocked by the HPA overloading, thus reducing the surface area and consequently the catalytic activity.

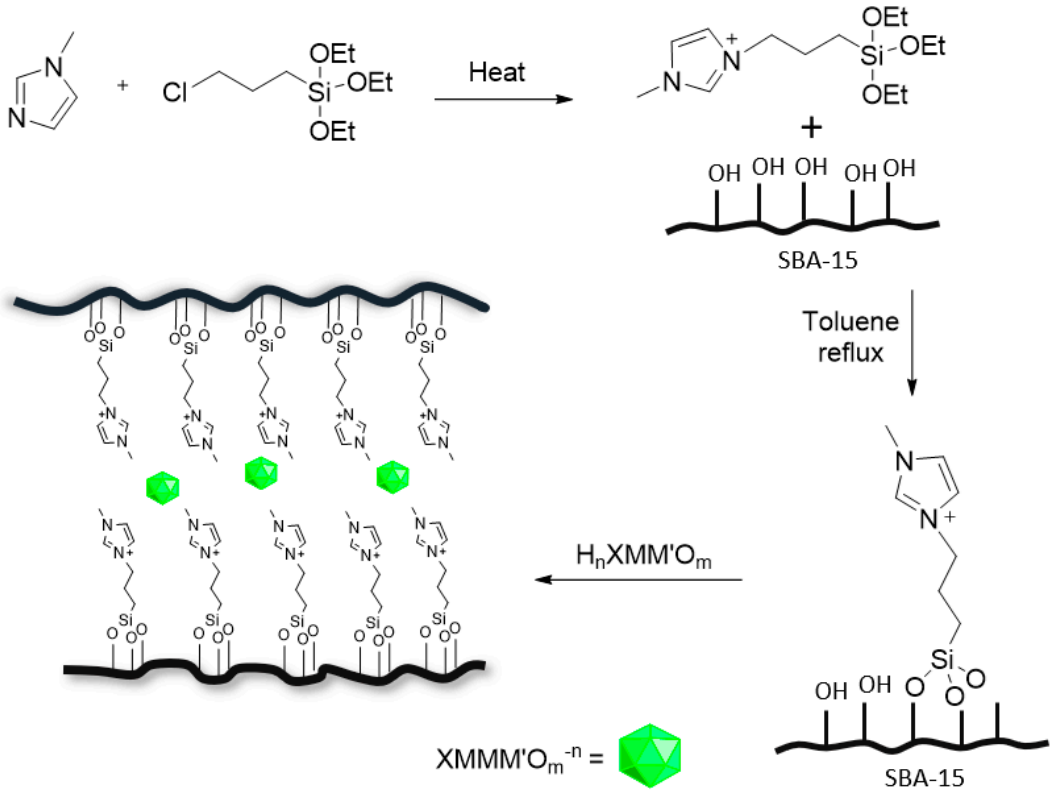

Figure 11. Synthetic route for the preparation of HPA immobilized over IL-SBA-15.

8.2. Phosphotungstic Containing POMs

Since the last fifteen years, several articles reported the preparation of heterogeneous catalysts based on the simple wet impregnation of variable amounts of phosphotungstic acid over mesoporous SBA-15 or mixed HY-SBA-15 composite zeolite [194], with the aim to study their catalytic activity in the ODS process applied either to model fuels [195] or real feeds [196] with H_2O_2, TBHP o air [197] as main oxidants. In general, these catalytic systems showed high activity and stability, being possible to reuse the heterogeneous catalysts after the regeneration step. Supports based on commercial silica showed worst results in comparison with mesoporous SBA-15, with the same tungsten loading, thus evidencing the positive role on the use of a mesoporous support allowing on the one hand the presence of well-dispersed tungsten species and on the other reducing the possible catalyst deactivation caused by sulfone deposition during oxidation. Nevertheless, some problems remain in SBA-15-supported catalysts being possible that phosphotungstic acids easily leached into a solution because of the weak interaction between them and SBA-15. Therefore, the search for catalysts with high activity and good recovery remains essential. From this point of view, the creativity of the researchers to find innovative solutions, ranged from the preparation of micro-mesoporous composite molecular sieves (ZSM-5/SBA-15) doped with different metal ions as Zr, Ag, Ce, thus balancing advantages/disadvantages of both types of supports [198] to the immobilization of phosphotungstic acids (HPW) onto composite supports as pentaethylenehexaamine (PEHA)-preloaded acidic Zr/SBA-15 with short pore channels [199]. In the latter, the synergic role of the zirconium-ion-modified acidic SBA-15 and the auxiliary PEHA molecules toward the high dispersion and stabilization of HPW clusters is believed to endow the resulting nanocomposites with high reusability in comparison to the zirconium free materials. A deep investigation on the potential effects of the preparation methods of

mesoporous HPW/SBA-15 catalysts on their catalytic performances on the ODS of a model oil, has been reported [200]. In this work, authors focused their study on two kind of catalysts prepared through silica aminofunctionalization (AF) or evaporation-induced self-assembly (EISA) methods, respectively (Figure 12). The study revealed that the catalyst prepared by EISA method gave better results, in terms of higher catalytic activity and stability in comparison with that obtained by AF procedure. The reasons may be found on the fact that, according to structural and spectroscopic analyses, in the first case the catalyst maintain the Keggin structure of original HPW molecules and has a high surface area; in the second strategy, the mesostructure of SBA-15 resulted partially blocked after the introduction of HPW molecules, and the Keggin structure of HPW molecules was damaged.

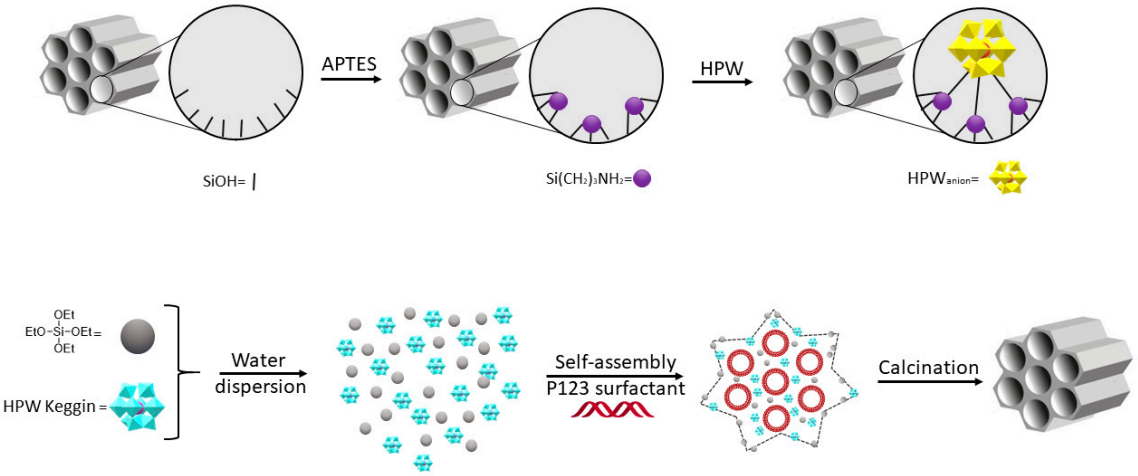

Figure 12. HPA immobilization strategies: through amino post- synthetic derivatization of SBA-15 (above) or by surfactant mediated self-assembly (below).

Anyway, the easy modification of native SBA-15 surface through a post-grafting procedure, in order to introduce more robust functional group (i.e., APTES to give H_2N-SBA-15 or *N*-(3-trimethoxysilylpropyl) tributylammonium to give tba-SBA-15) for the anchoring of different types of HPAs, justifies the large number of published articles appeared in literature, in the last decade. Among them, H_2N-SBA-15 and tba-SBA-15 supports were used to heterogenize, through an impregnation method, Keggin-type derivatives like lacunar polyanions $[PW_{11}O_{39}]^{7-}$ (PW_{11}), resulting by the removal of one WO^{4+} unit, or sandwich-type $[Eu(PW_{11}O_{39})_2]^{11-}$ anion affording robust and active catalysts for the ODS of model oil and real diesel, either under biphasic (diesel/acetonitrile 1:1) or solvent-free conditions [201,202]. Noteworthy, the PW_{11}/H_2N-SBA-15 composite system showed to maintain its activity for eight consecutive cycles. In another case, the amino functionalization of SBA-15 has been obtained either by one-step synthesis (co-condensation method, that is introducing the APTES into mesoporous silica in the presence of copolymer Pluronic P123) [203] or by the classical post-grafting procedure [204], having in mind the heterogenization, in both cases, of the Keggin-type 12-tungstophosphoric $[PW_{12}O_{40}]^{3-}$ HPA. In this case, the heterogeneous catalysts have been only used for the study of model oils with H_2O_2.

Composite catalysts based on tricopper(II)-substituted sandwich-type polyoxotungstates, having the general formula ($Cu_3X_2W_{18}$, X = Bi^{III}, Sb^{III}) supported over H_2N-SBA-15, have been prepared to be used in the H_2O_2 promoted ODS of thiophene [205]. Authors suggested that the best detected loading amount of $Cu_3X_2W_{18}$ species over the mesoporous silica was up to 4.7%, while worst activities were observed for higher levels of active species, as a result of the decreasing of surface area and pore diameters, thus hindering the flow of the reaction substrates into the pore channel of H_2N-SBA-15. No relevant differences, on the catalytic activity, have been detected for the two different polyoxotungstates containing Bi^{III} or Sb^{III}, respectively. In a recent paper, a contribution based on the use of a composite material formed by a phosphorous-containing tetranuclear peroxotungstate

$\{PO_4[WO_2(O_2)_2]_4\}^3$ Venturello anion symbolized as PW_4, immobilized on trimethylammonium functionalized SBA-15 (PW_4/tma-SBA-15) through an impregnation method, employed as catalyst for the ODS of model and real fuels, has been published [206]. Impressive data concerning activity and stability of heterogenized POM, have been reported by authors; moreover, carefully investigations on the fresh heterogeneous catalyst and on the material recovered after the successive recycling steps, showed that during the heterogenization and oxidation experiments an equilibrium between the two species PW_4 and the α-Keggin heteropolyanion $[PW_{12}O_{40}]^{3-}$ (PW_{12}), cannot be ruled out.

Accordingly to what above reported for the immobilization of phosphomolybdic based POMs, several authors published examples describing the preparation of phosphotungstic acid immobilized over ionic liquid-modified SBA-15 support too, having in mind to enhance the stability and the performances of the catalyst system. An interesting paper described the preparation of a series of hybrid polyoxometalates formed by the same anion α-Keggin phosphotungstate PW_{12} and three different ionic liquid cations, namely 1-butyl-3-methylimidazolium (BMIM), 1-butylpyridinium (BPy) and hexadecylpyridinium (HDPy), having the general formula $[IL]_3PW_{12}$ [207]. The activity and stability of these catalysts toward the ODS of model diesel under extractive conditions (ECODS), that is using $[BMIM]PF_6$ or acetonitrile as extraction solvent, have been studied in comparison with the phosphotungstate PW_{12} anion immobilized over the functionalized mesoporous tma-SBA-15 (see above). The latter (PW_{12}/tma-SBA-15) showed to be the most stable composite system having similar catalytic performances with the three homogeneous $[IL]_3PW_{12}$ catalysts and comparable activity both in acetonitrile and $[BMIM]PF_6$, even if with high recycling capacity. On the other hand, the classical ionic liquid derivatization of SBA-15, based on the preparation of the appropriate precursor 1-Methyl-3-(triethoxysilylpropyl)-imidazolium chloride ([pmim]Cl) ionic liquid and on the next grafting of the latter on SBA-15, allowed the anchoring of different HPA, ranging from the silicotungstic acid $H_4[SiO_4(W_3O_9)_4]$ [208] to the classical phosphotungstic PW_{12} anion [209]. In both cases, irrespective to the specific type of polyoxometalate composition, the anchoring on the IL functionalized support gave a system with higher catalytic activity for the H_2O_2 promoted ODS of model oils in comparison to the system obtained by unmodified SBA-15. As outlined by the authors, the reasons may be found on the enhanced wettability for the model oil promoted by the IL functionalization of the SBA-15 (changing its nature from hydrophilic to hydrophobic support), thus affording a catalytic system with high surface area, high accessibility of substrate and oxidant toward the active sites and substantially no leaching of the active species in the reaction mixture. Finally, the loading amount of HPA need to be carefully evaluated because beyond a certain value that varies for each species, the sulfur removal efficiency decrease due to the occurrence of mass transfer problems caused by the decrease of surface area and pore size of the support, thus limiting the successful contact between the substrates and the active species.

9. Miscellanea

In close correlation with SBA-15, the SBA-16 material is characterized by a more ordered three-dimensional (3-D) cage-like mesoporous structure, representing a further major achievement in the synthesis of mesoporous materials [210]. Pluronic F127 is used as a template to synthesize SBA-16 instead of P123 [211], providing larger pore diameter and wall thickness, as well as, higher thermal and hydrothermal stability [212]. Unfortunately, the preparation of SBA-16 requires acid conditions which are not compatible with the incorporation of a large panel of metal derivatives by traditional procedures, due to the occurrence of leaching processes. To avoid this drawback, Ti-SBA-16 mesoporous catalysts have been prepared (with various Ti loadings of 5, 10, and 15 wt%) by the evaporation-induced self-assembly method, and successively applied in the ODS procedure [213]. In this procedure, F127 in ethanol was treated with the appropriate amount of tetrabutyl titanate and TEOS under acid conditions (pH 2), followed by removal of the organic solvent and calcination at high temperature. Ti-SBA-16 showed the typical XRD signals of mesostructured material characterized by a slightly disordered structure. The presence of the silica-titanium framework was unambiguously

confirmed by FTIR analysis [214] and XPS analysis, this latter highlighting that all Ti ions were incorporated onto the SiO_2 structural motif [215–217]. Irrespective from the value of the Ti loading factor, all catalysts demonstrated a high activity in the oxidation of DBT as a model compound in n-octane/MeOH at 60 °C, using H_2O_2 as primary oxidant. A slight decrease in the activity of the catalysts was observed only at the highest 15 wt/% of Ti loading, probably due to the presence of major distortion effects on the mesoporous framework. Under optimal experimental conditions (that is 10 wt/% Ti-SBA-16, 60 °C for 3 h) 99% of sulfur removal was obtained.

10. Conclusions

The best catalysts and experimental conditions for the desulfurization process are summarized in Table 1, where the selection criteria have been focused upon the nature of the catalyst modification, the operating conditions and the percentage of the sulfur removal. As a general trend, the wetness impregnation and the grafting insertion technologies showed a similar efficacy in the activity of SBA-15 based metal oxide catalysts, with the only exception of TiO_2, in which case the grafting procedure yielded the most reactive system. The low expensive, mild and environmentally friendly H_2O_2 was applied as main oxidant in most of the reported procedure, highlighting the high catalytic performance of the metal oxides. The use of ionic liquids as selective extraction solvent or, in alternative, the employment of carboxylic acid as co-oxidant, does not appear to significantly improve the efficiency of the desulfurization process, with respect to simpler procedures. Among the metal oxides, V_2O_5/SBA-15 was the only catalyst able to activate dioxygen (even if at relatively high temperature, 120 °C), while [pmim] $FeCl_4$/SBA-15 was operative at the lowest reaction temperature (30 °C). With respect to the recyclability of the systems, Fe/SBA-15, TiO_2/SiO_2 and V_2O_5/SBA-15, were effective systems ranging from 4 to 5 and 6 successive runs, respectively. In the case of SBA-15 based polyoxometalates, wet impregnation or self-assembly strategies were the mainly used strategies for their heterogenization, varying from phosphomolybdic to phosphotungstic containing systems. Excellent results in terms of sulfur removal percentage and recyclability efficiencies have been observed after the POMs heterogenization on previously functionalized SBA-15, through the introduction of amino groups, trialkylammonium moieties or selected ionic liquids, even if excellent results were observed after simple doping of micro-mesoporous composite molecular sieves (ZSM-5/SBA-15) with Zr, Ag and Ce metal ions.

Table 1. Selection of optimal catalyst modification and operating conditions for SBA-15 anchored metal containing catalysts in the oxidative desulfurization process.

Catalyst Modification	Operating Conditions [a]	Sulfur Removal (%) [b]	Catalyst Recycle (n° of Runs) [c]	Reference
TiO_2/SiO_2 sol-gel method	BT, DBT, MDBT, and DMDBT, UV-irrad., air, toluene/dodecane, 25 °C, 2 h.	n.c.	5	[78]
TiO_2/SBA-15 grafting insertion	BT, DBT, 4-MDBT, and 4,6-DMDBT, CHP, n-heptane/toluene, 80 °C.	>99	n.a.	[91]
V_2O_5/SBA-15 wetness impregnation	Selective extraction phase DBT, 4-MDTB, 4,6-DMDTB, [Bmim]BF_4, O_2, 120 °C, 6 h.	99	6	[116]
CoMo/SBA-15 wetness impregnation	DBT, hexadecane, H_2O_2, 60 °C, 1 h.	90	n.a.	[125]
MoO_3/SBA-15 wetness impregnation	Formic acid as co-oxidant species, 4,6-DMDBT, H_2O_2, hexadecane, 70 °C, 1 h.	99	n.a.	[130]
[pmim]$FeCl_4$/SBA-15 grafting insertion	BT and DBT, H_2O_2, octane, 30 °C, 1 h.	94.3	n.a.	[137]
Fe/SBA-15 wetness impregnation	BT, DBT and 4,6-DMDBT, H_2O_2, n-dodecane and CH_3CN, 60 °C, 15 min.	90	4	[139]
WOx/SBA-15 grafting insertion	DBT, H_2O_2, n-dodecane, 100 °C, 2 h.	>99	n.a.	[155]
MoV/Zr/SBA-15 wetness impregnation	DBT, TBHP, n-hexane, 60 °C, 75 min.	98.5	4	[187]

Table 1. *Cont.*

Catalyst Modification	Operating Conditions [a]	Sulfur Removal (%) [b]	Catalyst Recycle (n° of Runs) [c]	Reference
$Cs_2Mo_8W_4$/SBA-15 wetness impregnation	DBT, TBHP, n-hexane, 60 °C, 80 min.	>99	4	[189]
HPMo/IL-SBA-15 wetness impregnation	DBT, H_2O_2, n-octane, 60 °C, 90 min.	>90	5	[193]
HPW/PEHA/Zr/SBA-15 layer by layer strategy	DBT, H_2O_2, n-octane, 60 °C, 60 min.	95	6	[199]
HPW/SiO_2-EISA self-assembly	BT, DBT and 4,6-DMDBT, H_2O_2, petroleum ether/CH_3CN, 60 °C, 2 h	>99	7	[200]
PW_{11}/H_2N-SBA-15 wetness impregnation	BT, DBT, 4-MDBT and 4,6-DMDBT, H_2O_2, n-octane and CH_3CN, 70 °C, 60 min.	>99	8	[201]
PW_4/tma-SBA-15 wetness impregnation	BT, DBT and 4,6-DMDBT, H_2O_2, n-octane and [Bmim]PF6 or MeCN, 70 °C, 3 h	>99	10	[206]
HSiW/IL-SBA-15 wetness impregnation	BT, DBT and 4,6-DMDBT, H_2O_2, n-octane, 60 °C, 2 h	96	8	[208]
TiO_2/SBA-16 self-assembly	DBT, n-octane, 60 °C, 3 h	>99	5	[213]

[a] BT:benzothiophene; DBT: dibenzothiophene; 4-MDBT: 4-methyldibenzothiophene; 4,6-DMDBT: 4,6- dimethyl dibenzothiophene. CHP: cumene hydroperoxide. [Bmim]BF_4: 1-butyl-3-methylimidazolium tetrafluoroborate. [pmim]: 1-methyl-3-(trimethoxysilylpropyl)-imidazolium. [b] n.c.: percentage of S removal, not calculated. [c] n.a.: not available.

Author Contributions: Conceptualization, writing—review and editing, M.C. and R.S.; graphics editing and literature review, B.M.B.

Funding: This work was supported by MIUR (Ministero dell'Istruzione, dell'Università della Ricerca Italiano), PRIN 2017 project "ORIGINALE CHEMIAE in Antiviral Strategy—Origin and Modernization of Multi-Component Chemistry as a Source of Innovative Broad Spectrum Antiviral Strategy", cod. 2017BMK8JR_002.

Conflicts of Interest: The authors declare no conflict of interest.

References

1. Dos Santos, S.M.L.; Nogueira, K.A.B.; De Souza Gama, M.; Lima, J.D.F.; Da Silva Júnior, I.J.; De Azevedo, D.C.S. Synthesis and characterization of ordered mesoporous silica (SBA-15 and SBA-16) for adsorption of biomolecules. *Microporous Mesoporous Mater.* **2013**, *180*, 284–292. [CrossRef]
2. Gaffar, I.; Rajamanickam, M. Mn-incorporated SBA-1 cubic mesoporous silicates: Synthesis and characterization. *Mater. Chem. Phys.* **2015**, *161*, 237–242.
3. Chaudhary, V.; Sharma, S. An overview of ordered mesoporous material SBA-15: Synthesis, functionalization and application in oxidation reactions. *J. Porous Mater.* **2017**, *24*, 741–749. [CrossRef]
4. Zhao, D.; Sun, J.; Li, Q.; Stucky, G.D. Morphological control of highly ordered mesoporous silica SBA-15. *Chem. Mater.* **2000**, *12*, 275–279. [CrossRef]
5. Shen, S.; Chen, F.; Chow, P.S.; Phanapavudhikul, P.; Zhu, K.; Tan, R.B.H. Synthesis of SBA-15 mesoporous silica via dry-gel conversion route. *Microporous Mesoporous Mater.* **2006**, *92*, 300–308. [CrossRef]
6. Zhao, D.; Feng, J.; Huo, Q.; Melosh, N.; Fredrickson, G.H.; Chmelka, B.F.; Stucky, G.D. Triblock copolymer syntheses of mesoporous silica with periodic 50 to 300 angstrom pores. *Science* **1998**, *279*, 548–552. [CrossRef]
7. Zhang, F.; Yan, Y.; Yang, H.; Meng, Y.; Yu, C.; Tu, B.; Zhao, D. Understanding effect of wall structure on the hydrothermal stability of mesostructured silica SBA-15. *J. Phys. Chem. B* **2005**, *109*, 8723–8732. [CrossRef]
8. Miyazawa, K.; Inagaki, S. Control of the microporosity within the pore walls of ordered mesoporous silica SBA-15. *Chem. Commun.* **2000**, *21*, 2121–2122. [CrossRef]
9. Yang, L.; Qi, Y.; Yuan, X.; Shen, J.; Kim, J. Direct synthesis, characterization and catalytic application of SBA-15 containing heteropolyacid $H_3PW_{12}O_{40}$. *J. Mol. Catal. A* **2005**, *229*, 199–205. [CrossRef]
10. Mohammadi Ziarani, G.; Lashgari, N.; Badiei, A. Application of Organoamine-functionalized Mesoporous Silica (SBA-Pr-NH2) as a Nano Base Catalyst in Organic Reactions. *Curr. Org. Chem.* **2017**, *21*, 674–687. [CrossRef]

11. Wu, S.H.; Lin, H.P. Synthesis of mesoporous silica nanoparticles. *Chem. Soc. Rev.* **2013**, *42*, 3862–3875. [CrossRef] [PubMed]
12. Hoffmann, F.; Cornelius, M.; Morell, J.; Fröba, M. Silica-based mesoporous organic-inorganic hybrid materials. *Angew. Chem. Int. Ed.* **2006**, *45*, 3216–3251. [CrossRef] [PubMed]
13. Martinez, F.; Han, Y.J.; Stucky, G.; Sotelo, J.L.; Ovejerob, G.; Melero, J.A. Synthesis and characterisation of iron-containing SBA-15 mesoporous silica. *Stud. Surf. Sci. Catal.* **2002**, *142*, 1109–1116.
14. García-Martínez, J.C.; González Uribe, H.A.; González-Brambila, M.M.; Colín-Luna, J.A.; Escobedo-García, Y.E.; López-Gaona, A.; Alvarado-Perea, L. Selective adsorption of nitrogen compounds using silica-based mesoporous materials as a pretreatment for deep hydrodesulfurization. *Catal. Today* **2018**, *305*, 40–48. [CrossRef]
15. Luan, Z. Alumination and ion exchange of mesoporous SBA-15 molecular sieves. *Chem. Mater.* **1999**, *11*, 1621–1627. [CrossRef]
16. Venezia, A.M.; Di Carlo, G.; Liotta, L.F.; Pantaleo, G.; Kantcheva, M. Effect of Ti(IV) loading on CH_4 oxidation activity and SO_2 tolerance of Pd catalysts supported on silica SBA-15 and HMS. *Appl. Catal. B* **2011**, *6*, 529–539. [CrossRef]
17. Mishra, G.S.; Machado, K.; Kumar, A. Highly selective n-alkanes oxidation to ketones with molecular oxygen catalyzed by SBA-15 supported rhenium catalysts. *J. Ind. Eng. Chem.* **2014**, *20*, 2228–2235. [CrossRef]
18. Hu, J.; Li, K.; Li, W.; Ma, F.; Guo, Y. Selective oxidation of styrene to benzaldehyde catalyzed by Schiff base-modified ordered mesoporous silica materials impregnated with the transition metal-monosubstituted Keggin-type polyoxometalates. *Appl. Catal. A* **2009**, *364*, 211–220. [CrossRef]
19. Yang, Y.; Zhang, Y.; Hao, S.; Guan, J.; Ding, H.; Shang, F.; Qiu, P.; Kan, Q. Heterogenization of functionalized Cu(II) and VO(IV) Schiff base complexes by direct immobilization onto amino-modified SBA-15: Styrene oxidation catalysts with enhanced reactivity. *Appl. Catal. A* **2010**, *381*, 274–281. [CrossRef]
20. Jin, M.; Kim, J.H.; Kim, J.M.; Jeon, J.K.; Jurng, J.; Bae, G.N.; Park, Y.K. Benzene oxidation with ozone over MnO_x/SBA-15 catalysts. *Catal. Today* **2013**, *204*, 108–113. [CrossRef]
21. Neeli, C.K.P.; Narani, A.; Marella, R.K.; Rao, K.S.R.; Burri, D.R. Selective benzylic oxidation of alkylaromatics over Cu/SBA-15 catalysts under solvent-free conditions. *Catal. Commun.* **2013**, *39*, 5–9. [CrossRef]
22. Cruz, P.; Perez, Y.; Hierro, I.D.; Fajardo, M. Copper, copper oxide nanoparticles and copper complexes supported on mesoporous SBA-15 as catalyst in the selective oxidation of benzyl alcohol in acqueous phase. *Microporous Mesoporous Mater.* **2016**, *220*, 136. [CrossRef]
23. Liotta, L.F.; Pantaleo, G.; Puleo, F.; Venezia, A.M. Au/CeO_2-SBA-15 catalysts for CO oxidation: Effect of ceria loading on physic-chemical properties and catalytic performances. *Catal. Today* **2012**, *187*, 10–19. [CrossRef]
24. Zhang, L.X.; Shi, J.L.; Yu, J.; Hua, Z.L.; Zhao, X.G.; Ruan, M.L. A new in-situ reduction route for the synthesis of Pt nanoclusters in the channels of mesoporous silica SBA-15. *Adv. Mater.* **2002**, *14*, 1510–1513. [CrossRef]
25. Xueguang, W.; Kyle, S.K.L.; Jerry, C.C.; Soofin, C. Direct Synthesis and Catalytic Applications of Ordered Large Pore Aminopropyl-Functionalized SBA-15 Mesoporous Materials. *J. Phys. Chem.* **2005**, *109*, 1763–1769.
26. Haribandhu, C.; Subhajit, D.; Ashis, S. Synthesis and use of SBA-15 adsorbent for dye-loaded wastewater treatment. *J. Environ. Chem. Eng.* **2015**, *3*, 2866–2874.
27. Tummino, M.L.; Testa, M.L.; Malandrino, M.; Gamberini, R.; Prevot, A.B.; Magnacca, G.; Laurenti, E. Green Waste-Derived Substances Immobilized on SBA-15 Silica: Surface Properties, Adsorbing and Photosensitizing Activities towards Organic and Inorganic Substrates. *Nanomaterials* **2019**, *9*, 162. [CrossRef] [PubMed]
28. Moritz, M.; Łaniecki, M. Application of SBA-15 mesoporous material as the carrier for drug formulation systems. Papaverine hydrochloride adsorption and release study. *Powder Technol.* **2012**, *230*, 106–111. [CrossRef]
29. Szewczyk, A.; Prokopowicz, M. Amino-modified mesoporous silica SBA-15 as bifunctional drug delivery system for cefazolin: Release profile and mineralization potential. *Mater. Lett.* **2018**, *227*, 136–140. [CrossRef]
30. EU Regulations. Available online: http://www.dieselnet.com/standards/eu/fuel.php (accessed on 3 June 2013).
31. Sharipov, A.K.; Nigmatullin, V.R. Removal of Sulfur from Hydrotreated Diesel Fuel. *Chem. Technol. Fuels Oils* **2005**, *41*, 225–229. [CrossRef]
32. González-García, O.; Cedeño-Caero, L. V-Mo based catalysts for oxidative desulfurization of diesel fuel. *Catal. Today* **2009**, *148*, 42–48. [CrossRef]
33. Rezvani, M.A.; Shaterian, M.; Aghbolagh, Z.S.; Babaei, R. Oxidative desulfurization of gasoline catalyzed by IMID@PMA@CS nanocomposite as a high-performance amphiphilic nano catalyst. *Environ. Prog. Sustain. Energy* **2018**, *37*, 1891–1900. [CrossRef]

34. Rezvani, M.A.; Shaterian, M.; Akbarzadeh, F.; Khandan, S. Deep oxidative desulfurization of gasoline induced by PMoCu@$MgCu_2O_4$-PVA composite as a high-performance heterogeneous nanocatalyst. *Chem. Eng. J.* **2018**, *333*, 537–544. [CrossRef]
35. Eßer, J.; Wasserscheid, P.; Jess, A. Deep desulfurization of oil refinery streams by extraction with ionic liquids. *Green Chem.* **2004**, *6*, 316–322. [CrossRef]
36. Zeelani, G.G.; Lal Pal, S. A Review on Desulfurization Techniques of Liquid Fuels. *Int. J. Sci. Res.* **2016**, *5*, 2413–2419.
37. Vsudevan, P.T.; Fierro, J.L.G. A Review of Deep Hydrodesulfurization Catalysis. *Catal. Rev. Sci. Eng.* **1996**, *38*, 2. [CrossRef]
38. Tanimu, A.; Alhooshani, K. Advanced Hydrodesulfurization Catalysts: A Review of Design and Synthesis. *Energy Fuels* **2019**, *33*, 2810–2838. [CrossRef]
39. Huirache-Acuña, R.; Rufino, N.; Peza-Ledesma, C.L.; Javier, L.R.; Alonso-Núñe, G.; Pawelec, B.; Rivera-Muñoz, E.M. SBA-15 Mesoporous Silica as Catalytic Support for Hydrodesulfurization Catalysts-Review. *Materials* **2013**, *6*, 4139–4167. [CrossRef]
40. Oyama, S.T.; Zhao, H.; Freund, H.J.; Asakura, K.; Włodarczyk, R.; Sierka, M. Unprecedented selectivity to the direct desulfurization (DDS) pathway in a highly active FeNi bimetallic phosphide catalyst. *J. Catal.* **2012**, *285*, 1–5. [CrossRef]
41. Jiang, Z.X.; Liu, Y.; Sun, X.P.; Tian, F.P.; Sun, F.X.; Liang, C.H.; You, W.S.; Han, C.R.; Li, C. Activated Carbons Chemically Modified by Concentrated H_2SO_4 for the Adsorption of the Pollutants from Wastewater and the Dibenzothiophene from Fuel Oils. *Langmuir* **2003**, *19*, 731–736. [CrossRef]
42. Al-Shahrani, F.; Xiao, T.; Llewellyn, S.A.; Barri, S.; Jiang, Z.; Shi, H.; Martinie, G.; Green, M.L.H. Desulfurization of diesel via the H_2O_2 oxidation of aromatic sulfides to sulfones using a tungstate catalyst. *Appl. Catal. B.* **2007**, *73*, 311–316. [CrossRef]
43. Babich, I.V.; Moulijn, J.A. Science and technology of novel processes for deep desulfurization of oil refinery streams: A review. *Fuel* **2003**, *82*, 607–631. [CrossRef]
44. Schulz, H.; Böhringer, W.; Waller, P.; Ousmanov, F. Gas oil deep hydrodesulfurization: Refractory compounds and retarded kinetics. *Catal. Today* **1999**, *49*, 87–97. [CrossRef]
45. Dou, S.-Y.; Wang, R. Recent Advances in New Catalysts for Fuel Oil Desulfurization. *Curr. Org. Chem.* **2017**, *21*, 1019–1036. [CrossRef]
46. Zhu, W.; Li, H.; Jiang, X.; Yan, Y.; Lu, J.; Xia, J. Oxidative Desulfurization of Fuels Catalyzed by Peroxotungsten and Peroxomolybdenum Complexes in Ionic Liquids. *Energy Fuels* **2007**, *21*, 2514–2516. [CrossRef]
47. Saladino, R.; Botta, G.; Crucianelli, M. Advances in Nanostrostructured Transition Metal Catalysis Applied to Oxidative Desulfurization. In *Applying Nanotechnology to the Desulfurization Process in Petroleum Engineering*; Saleh, T.A., Ed.; IGI Global, 2016; pp. 1–555.
48. Liu, Y.-Y.; Leus, K.; Sun, Z.; Li, X.; Depauw, H.; Wang, A.; Zhang, J.; Van Der Voort, P. Catalytic oxidative desulfurization of model and real diesel over a molybdenum anchored metal-organic framework. *Microporous Mesoporous Mat.* **2019**, *277*, 245–252. [CrossRef]
49. Chan, N.Y.; Lin, T.-Y.; Yen, T.F. Superoxides: Alternative Oxidants for the Oxidative Desulfurization Process. *Energy Fuels* **2008**, *22*, 3326–3328. [CrossRef]
50. Shaabani, A.; Behnam, M.; Rezayan, A.H. Tungstophosphoric Acid ($H_3PW_{12}O_{40}$) Catalyzed Oxidation of Organic Compounds with $NaBrO_3$. *Catal. Commun.* **2009**, *10*, 1074–1078. [CrossRef]
51. Campos-Martin, J.M.; Capel-Sanchez, M.C.; Fierro, J.L.G. Highly efficient deep desulfurization of fuels by chemical oxidation. *Green Chem.* **2004**, *6*, 557–562. [CrossRef]
52. Garcìa-Gutiérrez, J.L.; Fuentes, G.A.; Hernàndez-Teràn, M.E.; Murrieta, F.; Navarrete, J.; Jiménez-Cruz, F. Ultra-deep oxidative desulfurization of diesel fuel with H_2O_2 catalyzed under mild conditions by polymolybdates supported on Al_2O_3. *Appl. Catal.* **2006**, *305*, 15–20. [CrossRef]
53. Ciclosi, M.; Dinoi, C.; Gonsalvi, L.; Peruzzini, M.; Manoury, E.; Poli, R. Oxidation of Thiophene Derivatives with H_2O_2 in Acetonitrile Catalyzed by [Cp*2M_2O_5] (M = Mo, W): A Kinetic Study. *Organometallics* **2008**, *27*, 2281–2286. [CrossRef]
54. Liu, G.; Cao, Y.; Jiang, R.; Wang, L.; Zhang, X.; Mi, Z. Oxidative desulfurization of jet fuels and its impact on thermal-oxidative stability. *Energy Fuel* **2009**, *23*, 5978–5985. [CrossRef]
55. Noyori, R.; Aoki, M.; Sato, K. Green oxidation with aqueous hydrogen peroxide. *Chem. Commun.* **2003**, 1977–1986. [CrossRef] [PubMed]

56. Maksimchuk, N.; Lee, J.S.; Ayupov, A.; Chang, J.-S.; Kholdeeva, O. Cyclohexene Oxidation with H_2O_2 over Metal-Organic Framework MIL-125(Ti): The Effect of Protons on Reactivity. *Catalysts* **2019**, *9*, 324. [CrossRef]
57. Di Giuseppe, A.; Crucianelli, M.; De Angelis, F.; Crestini, C.; Saladino, R. Efficient Oxidation of Thiophene Derivatives with Homogeneous and Heterogeneous MTO/H_2O_2 systems: A novel approach for Oxidative Desulfurization (ODS) of Diesel Fuel. *Appl. Catal. B* **2009**, *89*, 239–245. [CrossRef]
58. Saladino, R.; Crucianelli, M.; De Angelis, F. Methyltrioxorhenium catalysis in nonconventional solvents: A great catalyst in safe reaction medium. *ChemSusChem* **2010**, *3*, 524–540.
59. Meman, N.M.; Pourkhalil, M.; Rashidi, A.; Zarenezhad, B. Synthesis, characterization and operation of a functionalized multi-walled CNT supported MnOx nanocatalyst for deep oxidative desulfurization of four petroleum fractions. *J. Ind. Eng. Chem.* **2014**, *20*, 4054–4058. [CrossRef]
60. Balzani, V.; Credi, A.; Venture, M. Photochemical conversion of solar energy. *ChemSusChem* **2008**, *1*, 26–58. [CrossRef]
61. Ramirez-Verduzco, L.F.; De los Reyes, J.A.; Torres-Garcia, E. Solvent Effect in Homogeneous and Heterogeneous Reactions to Remove Dibenzothiophene by an Oxidation-Extraction Scheme. *Ind. Eng. Chem. Res.* **2008**, *47*, 5353–5361. [CrossRef]
62. Rodríguez-Cabo, B.; Rodríguez, H.; Rodil, E.; Arce, A.; Soto, A. Extractive and oxidative-extractive desulfurization of fuels with ionic liquids. *Fuel* **2014**, *117*, 882–889. [CrossRef]
63. Taguchi, A.; Schuth, F. Ordered mesoporous materials in catalysis. *Microporous Mesoporous Mater.* **2005**, *77*, 1–45. [CrossRef]
64. Huang, D.; Wang, Y.J.; Cui, Y.C.; Luo, G.S. Direct synthesis of mesoporous TiO_2 and its catalytic performance in DBT oxidative desulfurization. *Microporous Mesoporous Mater.* **2008**, *116*, 378–385. [CrossRef]
65. Tanev, P.T.; Chibwe, M.; Pinnavaia, T.J. Titanium-containing mesoporous molecular sieves for catalytic oxidation of aromatic compounds. *Nature* **1994**, *368*, 321–323. [CrossRef]
66. Chica, A.; Corma, A.; Dómine, M.E. Catalytic oxidative desulfurization (ODS) of diesel fuel on a continuous fixed-bed reactor. *J. Catal.* **2006**, *242*, 299–308. [CrossRef]
67. Yan, X.M.; Mei, P.; Lei, J.; Mi, Y.; Xiong, L.; Guo, L. Synthesis and characterization of mesoporous phosphotungstic acid/TiO_2 nanocompositive as a novel oxidative desulfurization catalyst. *J. Mol. Chem. Catal. A Chem.* **2009**, *304*, 52–57. [CrossRef]
68. Seung-Tae, Y.; Kwang-Eun, J.; Soon-Yong, J.; Wha-Seung, A. Synthesis of mesoporous TS-1 using a hybrid SiO_2-TiO_2 xerogel for catalytic oxidative desulfurization. *Mater. Res. Bull.* **2012**, *47*, 4398–4402.
69. Sengupta, A.; Kamble, P.D.; Basu, J.K.; Sengupta, S. Kinetic study and optimization of oxidative desulfurization of benzothiophene using mesoporous titanium silicate-1 catalyst. *Ind. Eng. Chem. Res.* **2012**, *51*, 147–157. [CrossRef]
70. Tangestaninejad, S.; Mirkhani, V.; Moghadam, M.; Mohammadpoor-Baltork, I.; Shams, E.; Salavati, H. Hydrocarbon oxidation catalyzed by vanadium polyoxometalate supported on mesoporous MCM-41 under ultrasonic irradiation. *Ultrason. Sonochem.* **2008**, *15*, 438–447. [CrossRef]
71. Chen, Y.; Zhang, F.; Fang, Y.; Zhu, X.; Zhen, W.; Wang, R.; Ma, J. Phosphotungstic acid containing ionic liquid immobilized on magnetic mesoporous silica rod catalyst for the oxidation of dibenzothiophene with H_2O_2. *Catal. Commun.* **2013**, *38*, 54–58. [CrossRef]
72. Wang, X.; Zhang, W.; Wu, L.; Ye, F.; Xiao, J.; Li, Z. One-pot photocatalysis-assisted adsorptive desulfurization of diesel over doped-TiO_2 under ambient conditions. *RSC Adv.* **2014**, *4*, 56567–56570. [CrossRef]
73. Shen, C.; Wang, Y.J.; Xu, J.H.; Luo, G.S. Synthesis of TS-1 on porous glass beads for catalytic oxidative desulfurization. *Chem Eng. J.* **2015**, *259*, 552–561. [CrossRef]
74. Sentorun-Shalaby, C.; Saha, S.K.; Ma, X.L.; Song, C.S. Mesoporous-molecular-sievesupported nickel sorbents for adsorptive desulfurization of commercial ultralow-sulfur diesel fuel. *Appl. Catal. B.* **2011**, *101*, 718–726. [CrossRef]
75. Ren, X.; Miao, G.; Xiao, Z.; Ye, F.; Li, Z.; Wang, H.; Xiao, J. Catalytic adsorptive desulfurization of model diesel fuel using TiO_2/SBA-15 under mild conditions. *Fuel* **2016**, *174*, 118–125. [CrossRef]
76. Hao, X.; Quach, L.; Korah, J.; Spieker, W.A.; Regalbuto, J.R. The control of platinum impregnation by PZC alteration of oxides and carbon. *J. Mol. Catal. A Chem.* **2004**, *219*, 97–107. [CrossRef]
77. Lee, K.X.; Valla, J.A. Adsorptive desulfurization of liquid hydrocarbons using zeolite-based sorbents: A comprehensive review. *React. Chem. Eng.* **2019**, *4*, 1357–1386. [CrossRef]

78. Miao, G.; Ye, F.; Wu, L.; Ren, X.; Xiao, J.; Li, Z.; Wang, H. Selective adsorption of thiophenic compounds from fuel over TiO_2/SiO_2 under UV-irradiation. *J. Hazard. Mater.* **2015**, *300*, 426–432. [CrossRef]
79. Rourke, C.O.; Bowler, D.R. Adsorption of thiophene-conjugated sensitizers on TiO_2 anatase (101). *J. Phys. Chem.* **2010**, *114*, 20240–20248.
80. Zhuravlev, L.T. Concentration of hydroxyl groups on the surface of amorphous silicas. *Langmuir* **1987**, *3*, 316–318. [CrossRef]
81. Collins, F.M.; Lucy, A.R.; Sharp, C. Oxidative desulphurization of oils via hydrogen peroxide and heteropolyanion catalysis. *J. Mol. Catal. A Chem.* **1997**, *117*, 397–403. [CrossRef]
82. Gao, G.; Cheng, S.; An, Y.; Si, X.; Fu, X.; Liu, Y.; Zhang, H.; Wu, P.; He, M.Y. Oxidative Desulfurization of Aromatic Sulfur Compounds over Titanosilicates. *ChemCatChem.* **2010**, *2*, 459–466. [CrossRef]
83. Capel-Sanchez, M.C.; Campos-Martin, J.M.; Fierro, J.L.G. Removal of refractory organosulfur compounds via oxidation with hydrogen peroxide on amorphous Ti/SiO_2 catalysts. *Energy Environ. Sci.* **2010**, *3*, 328–333. [CrossRef]
84. Bérubé, F.; Khadhraoui, A.; Janicke, M.T.; Kleitz, F.; Kaliaguine, S. Optimizing Silica Synthesis for the Preparation of Mesoporous Ti-SBA-15 Epoxidation Catalysts. *Ind. Eng. Chem. Res.* **2010**, *49*, 6977–6985. [CrossRef]
85. Berube', F.; Nohair, B.; Kleitz, F.; Kaliaguine, S. Controlled Postgrafting of Titanium Chelates for Improved Synthesis of Ti-SBA-15 Epoxidation Catalysts. *Chem. Mater.* **2010**, *22*, 1988–2000. [CrossRef]
86. Choi, M.; Heo, W.; Kleitz, F.; Ryoo, R. Facile synthesis of high quality mesoporous SBA-15 with enhanced control of the porous network connectivity and wall thickness. *Chem. Commun.* **2003**, 1340–1341. [CrossRef] [PubMed]
87. Kleitz, F.; Bérubé, F.; Guillet-Nicolas, R.; Yang, C.M.; Thommes, M. Probing Adsorption, Pore Condensation, and Hysteresis Behavior of Pure Fluids in Three-Dimensional Cubic Mesoporous KIT-6 Silica. *J. Phys. Chem. C* **2010**, *114*, 9344–9355. [CrossRef]
88. Cedeño-Caero, L.; Ramos-Luna, M.; Méndez-Cruz, M.; Ramírez-Solís, J. Oxidative desulfurization of dibenzothiophene compounds with titania based catalysts. *Catal. Today* **2011**, *172*, 189–194. [CrossRef]
89. Zhang, W.-H.; Lu, J.; Han, B.; Li, M.; Xiu, J.; Ying, P.; Can, L. Direct Synthesis and Characterization of Titanium-Substituted Mesoporous Molecular Sieve SBA-15. *Chem. Mater.* **2002**, *14*, 3413–3421. [CrossRef]
90. Kruk, M.; Jaroniec, M.; Ko, C.H.; Ryoo, R. Characterization of the Porous Structure of SBA-15. *Chem. Mater.* **2000**, *12*, 1961–1968. [CrossRef]
91. Kim, T.-W.; Kim, M.-J.; Kleitz, F.; Nair, M.M.; Guillet Nicolas, R.; Jeong, K.-E.; Chae, H.-J.; Kim, C.-U.; Jeong, S.-Y. Tailor-Made Mesoporous Ti-SBA-15 Catalysts for Oxidative Desulfurization of Refractory Aromatic Sulfur Compounds in Transport Fuel. *ChemCatChem* **2012**, *4*, 687–697. [CrossRef]
92. Bianconi, A.; Fritsch, E.; Calas, G.; Petiau, J. X-ray-absorption near-edge structure of 3d transition elements in tetrahedral coordination: The effect of bond-length variation. *Phys. Rev. B Condens. Matter.* **1985**, *32*, 4292–4295. [CrossRef]
93. Laredo, G.C.; Leyva, S.; Alvarez, R.; Mares, M.T.; Castillo, J.; Cano, J.L. Nitrogen compounds characterization in atmospheric gas oil and light cycle oil from a blend of Mexican crudes. *Fuel* **2002**, *81*, 1341–1350. [CrossRef]
94. Cho, K.-S.; Le, Y.-K. Effects of nitrogen compounds, aromatics, and aprotic solvents on the oxidative desulfurization (ODS) of light cycle oil over Ti-SBA-15 catalyst. *Appl. Catal. B* **2014**, *147*, 35–42. [CrossRef]
95. Ishihara, A.; Wang, D.; Dumeignil, F.; Amano, H.; Qian, E.W.; Kabe, T. Oxidative desulfurization and denitrogenation of a light gas oil using an oxidation/adsorption continuous flow process. *Appl. Catal. A* **2005**, *279*, 279–287. [CrossRef]
96. Caero, L.C.; Navarro, J.F.; Gutierrez-Alejandre, A. Oxidative desulfurization of synthetic diesel using supported catalysts: Part II. Effect of oxidant and nitrogen-compounds on extraction–oxidation process. *Catal. Today* **2006**, *116*, 562–568. [CrossRef]
97. Jia, Y.; Li, G.; Ning, G.; Jin, C. The effect of N-containing compounds on oxidative desulphurization of liquid fuel. *Catal. Today* **2009**, *140*, 192–196. [CrossRef]
98. Mirante, F.; Ribeiro, S.O.; De Castro, B.; Granadeiro, C.M.; Balula, S.S. Sustainable Desulfurization Processes Catalyzed by TitaniumPolyoxometalate@TM-SBA-15. *Top. Catal.* **2017**, *60*, 1140–1150. [CrossRef]
99. Kholdeeva, O.A.; Kovaleva, L.A.; Maksimovskaya, R.I.; Maksimov, G.M. Kinetics and mechanism of thioether oxidation with H_2O_2 in the presence of Ti (IV)-substituted heteropolytungstates. *J. Mol. Catal. A Chem.* **2000**, *158*, 223–229. [CrossRef]

100. Maksimov, G.M.; Maksimovskaya, R.I.; Kholdeeva, O.A.; Fedotov, M.A.; Zaikovskii, V.I.; Vasil'ev, V.G.; Arzumanov, S.S. Structure and properties of $H_8(PW_{11}TiO_{39})2O$ heteropoly acid. *J. Struct. Chem.* **2009**, *50*, 618–627. [CrossRef]
101. Balula, S.S.; Cunha-Silva, L.; Santos, I.C.M.S.; Estrada, A.C.; Fernandes, A.C.; Cavaleiro, J.A.S.; Pires, J.; Freire, C.; Cavaleiro, A.M.V. Mono-substituted silicotungstates as active catalysts for sustainable oxidations: Homo- and heterogeneous performance. *New J. Chem.* **2013**, *37*, 2341–2350. [CrossRef]
102. Balula, S.S.; Santos, I.C.M.S.; Cunha-Silva, L.; Carvalho, A.P.; Pires, J.; Freire, C.; Cavaleiro, J.A.S.; de Castro, B.; Cavaleiro, A.M.V. Phosphotungstates as catalysts for monoterpenes oxidation: Homo- and heterogeneous performance. *Catal. Today* **2013**, *203*, 95–102. [CrossRef]
103. Kholdeeva, O.A.; Maksimovskaya, R.I. Titanium- and zirconium-monosubstituted polyoxometalates as molecular models for studying mechanisms of oxidation catalysis. *J. Mol. Catal. A Chem.* **2007**, *262*, 7–24. [CrossRef]
104. Xu, J.; Zhao, S.; Chen, W.; Wang, M.; Song, Y.F. Highly efficient extraction and oxidative desulfurization system using $Na_7H_2LaW_{10}O_{36}{\cdot}32\ H_2O$ in $[bmim]BF_4$ at room temperature. *Chem. A Eur. J.* **2012**, *18*, 4775–4781. [CrossRef] [PubMed]
105. Zhu, W.; Huang, W.; Li, H.; Zhang, M.; Jiang, W.; Chen, G.; Han, C. Polyoxometalate-based ionic liquids as catalysts for deep desulfurization of fuels. *Fuel Process. Technol.* **2011**, *92*, 1842–1848. [CrossRef]
106. Caero, L.C.; Hernández, E.; Pedraza, F.; Murrieta, F. Oxidative desulfurization of synthetic diesel using supported catalysts: Part, I. Study of the operation conditions with a vanadium oxide based catalyst. *Catal. Today* **2005**, *107–108*, 564–569. [CrossRef]
107. Shiraishi, Y.; Naito, T.; Hirai, T. Vanadosilicate Molecular Sieve as a Catalyst for Oxidative Desulfurization of Light Oil. *Ind. Eng. Chem. Res.* **2003**, *42*, 6034–6039. [CrossRef]
108. Anisimov, A.V.; Fedorova, E.V.; Lesnugin, A.Z.; Senyavin, V.M.; Aslanov, L.A.; Rybakov, V.B.; Tarakanova, A.V. Vanadium peroxocomplexes as oxidation catalysts of sulfur organic compounds by hydrogen peroxide in bi-phase systems. *Catal. Today* **2003**, *78*, 319–325. [CrossRef]
109. Du, G.; Lim, S.; Pinault, M.; Wang, C.; Fang, F.; Pfefferle, L.; Haller, G.L. Synthesis, characterization, and catalytic performance of highly dispersed vanadium grafted SBA-15 catalyst. *J. Catal.* **2008**, *253*, 74–90. [CrossRef]
110. Cedeño-Caero, L.; Gomez-Bernal, H.; Fraustro-Cuevas, A.; Guerra-Gomez, H.D.; Cuevas-Garcia, R. Oxidative desulfurization of synthetic diesel using supported catalysts. Part III. Support effect on vanadium-based catalysts. *Catal. Today* **2008**, *133–135*, 244–254. [CrossRef]
111. Rivoira, L.; Martínez, M.L.; Anunziata, O.; Beltramone, A. Vanadium oxide supported on mesoporous SBA-15 modified with Al and Ga as a highly active catalyst in the ODS of DBT. *Microporous Mesoporous Mater.* **2017**, *254*, 96–113. [CrossRef]
112. Yang, P.; Zhao, D.; Chmelka, B.F.; Stucky, G.D. Triblock-copolymer-directed syntheses of large-pore mesoporous silica fibers. *Chem. Mater.* **1998**, *10*, 2033–2036. [CrossRef]
113. Liu, Y.M.; Cao, Y.; Yi, W.; Feng, W.L.; Dai, W.L.; Yan, S.R.; He, H.Y.; Fan, K.N. Vanadium oxide supported on mesoporous SBA-15 as highly selective catalysts in the oxidative dehydrogenation of propane. *J. Catal.* **2004**, *224*, 417–428. [CrossRef]
114. Kumar, R.; Sithambaram, S.; Suib, S.L. Cyclohexane oxidation catalyzed by manganese oxide octahedral molecular sieves-Effect of acidity of the catalyst. *J. Catal.* **2009**, *262*, 304–313. [CrossRef]
115. Rivoira, L.P.; Cussa, J.; Martínez, M.L.; Beltramone, A.R. Experimental design optimization of the ODS of DBT using vanadium oxide supported on mesoporous Ga-SBA-15. *Catal. Today* **2018**. [CrossRef]
116. Wang, C.; Chen, Z.; Yao, X.; Jiang, W.; Zhang, M.; Li, H.; Liu, H.; Zhu, W.; Li, H. One-pot extraction and aerobic oxidative desulfurization with highly dispersed V2O5/SBA-15 catalyst in ionic liquids. *RSC Adv.* **2017**, *7*, 39383. [CrossRef]
117. Gao, X.; Xu, J. The oxygen activated by the active vanadium species for the selective oxidation of benzene to phenol. *Catal. Lett.* **2006**, *111*, 203. [CrossRef]
118. Jia, Y.; Li, G.; Ning, G. Efficient oxidative desulfurization (ODS) of model fuel with H_2O_2 catalyzed by $MoO_3/\gamma\text{-}Al_2O_3$ under mild and solvent free conditions. *Fuel Process. Technol.* **2011**, *92*, 106–111. [CrossRef]
119. Hu, Z.; Lu, S.; Huang, X.; Li, J.; Duan, Y.; Yan, L.; Yao, Y.; Liao, X. Molybdenum anchored on NH_2-modified spherical SiO_2: A highly efficient and stable catalyst for oxidative desulfurization of fuel oil. *Appl. Organomet. Chem.* **2018**, *32*, e4521. [CrossRef]

120. Han, X.; Wang, A.; Wang, X.; Li, X.; Wang, Y.; Hu, Y. Catalytic performance of P-modified MoO_3/SiO_2 in oxidative desulfurization by cumene hydroperoxide. *Catal. Commun.* **2013**, *42*, 6–9. [CrossRef]
121. Chang, J.; Wang, A.; Liu, J.; Li, X.; Hu, Y. Oxidation of dibenzothiophene with cumene hydroperoxide on MoO_3/SiO_2 modified with alkaline earth metals. *Catal. Today* **2010**, *149*, 122–126. [CrossRef]
122. Shao, X.; Zhang, X.; Yu, W.; Wu, Y.; Qin, Y.; Sun, Z.; Song, L. Effects of surface acidities of MCM-41 modified with MoO_3 on adsorptive desulfurization of gasoline. *Appl. Surf. Sci.* **2012**, *263*, 1–7. [CrossRef]
123. Ramos, J.M.; Wang, J.A.; Chen, L.F.; Arellano, U.; Ramírez, S.P.; Sotelo, R.; Schachat, P. Synthesis and catalytic evaluation of CoMo/SBA-15 catalysts for oxidative removal of dibenzothiophene from a model diesel. *Catal. Commum.* **2015**, *72*, 57–62. [CrossRef]
124. La Parola, V.; Degnello, G.; Tewell, C.R.; Venrzial, A.M. Structural characterization of silica supported CoMo catalysts by UV, Raman spectroscopy, XPS and X-ray diffraction techniques. *Appl. Catal. A Gen.* **2002**, *235*, 171–180. [CrossRef]
125. Briggs, D.; Seah, M.P. (Eds.) *Practical Surface analysis, Auger and X-ray Photoelectron Spectroscopy*, 2nd ed.; Wiley: New York, NY, USA, 1990; p. 607.
126. González, J.; Wang, J.A.; Chen, L.; Manríquez, M.; Salmones, J.; Limas, R.; Arellano, U. Quantitative determination of oxygen defects, surface lewis acidity, and catalytic properties of mesoporous MoO_3/SBA-15 catalysts. *J. Solid State Chem.* **2018**, *263*, 100–111. [CrossRef]
127. Basahel, S.N.; Ali, T.T.; Narasimharao, K.; Bagabas, A.A.; Mokhtar, M. Effect of iron oxide loading on the phase transformation and physicochemical properties of nanosized mesoporous ZrO_2. *Mater. Res. Bull.* **2012**, *47*, 3463–3472. [CrossRef]
128. Epifani, M.; Imperatori, P.; Mirenghi, L.; Schioppa, M.; Siciliano, P. Synthesis and Characterization of MoO_3 Thin Films and Powders from a Molybdenum Chloromethoxide. *Chem. Mater.* **2004**, *16*, 5495–5501. [CrossRef]
129. He, T.; Yao, J. Photochromism of molybdenum oxide. *J. Photochem. Photobiol. C Photochem. Rev.* **2003**, *4*, 125–143. [CrossRef]
130. De Filippis, P.; Scarsella, M.; Verdone, N. Oxidative Desulfurization I: Peroxyformic Acid Oxidation of Benzothiophene and Dibenzothiophene. *Ind. Eng. Chem. Res.* **2009**, *48*, 1372–1375. [CrossRef]
131. Arends, I.W.C.E.; Sheldon, R.A. Activities and stabilities of heterogeneous catalysts in selectiveliquid phase oxidations: Recent developments. *Appl. Catal. A* **2001**, *212*, 175–187. [CrossRef]
132. Wang, Q.L.; Lei, L.C.; Zhu, J.K.; Yang, B.; Li, Z.J. Deep desulfurization of fuels by extraction with 4-dimethylaminopyridinium-based ionic liquids. *Energy Fuels* **2013**, *27*, 4617–4623. [CrossRef]
133. Chen, X.C.; Song, D.D.; Asumana, C.; Yu, G.R. Deep oxidative desulfurization of diesel fuels by Lewis acidic ionic liquids based on 1-n-butyl-3-methylimidazolium metal chloride. *J. Mol. Catal. A* **2012**, *359*, 8–13. [CrossRef]
134. Nie, Y.; Dong, Y.X.; Bai, L.; Dong, H.F.; Zhang, X.P. Fast oxidative desulfurization of fuel oil using dialkylpyridinium tetrachloroferrates ionic liquids. *Fuel* **2013**, *103*, 997–1002. [CrossRef]
135. Zhu, W.S.; Zhang, J.T.; Li, H.M.; Chao, Y.H.; Jiang, W.; Yin, S.; Liu, H. Fenton-like ionic liquids/H_2O_2 system: One-pot extraction combined with oxidation desulfurization of fuel. *RSC Adv.* **2012**, *2*, 658–664. [CrossRef]
136. Zhang, J.T.; Zhu, W.S.; Li, H.M.; Jiang, W.; Jiang, Y.Q.; Huang, W.L.; Yan, Y.S. Deep oxidative desulfurization of fuels by Fenton-like reagent in ionic liquids. *Green Chem.* **2009**, *11*, 1801–1807. [CrossRef]
137. Ding, W.; Zhu, W.; Xiong, J.; Yang, L.; Wei, A.; Zhang, M.; Li, H. Novel heterogeneous iron-based redox ionic liquid supported on SBA-15 for deep oxidative desulfurization of fuels. *Chem. Eng. J.* **2015**, *266*, 213–221. [CrossRef]
138. Bordoloi, A.; Sahoo, S.; Lefebvre, F.; Halligudi, S. Heteropoly acid-based supported ionic liquid-phase catalyst for the selective oxidation of alcohols. *J. Catal.* **2008**, *259*, 232–239. [CrossRef]
139. Rivoira, L.; Juárez, J.; Martínez, M.L.; Beltramone, A. Iron-modified mesoporous materials as catalysts for ODS of sulfur compounds. *Catal. Today* **2018**. [CrossRef]
140. Sanjini, N.S.; Velmathi, S. Iron impregnated SBA-15, a mild and efficient catalyst for the catalytic hydride transfer reduction of aromatic nitro compounds. *RSC Adv.* **2014**, *4*, 15381–15388. [CrossRef]
141. Chaliha, S.; Bhattacharyya, K.G. Fe(III)-, Co(II)- and Ni(II)-impregnated MCM41 for wet oxidative destruction of 2,4-dichlorophenol in water. *Catal. Today* **2009**, *141*, 225–233. [CrossRef]

142. Barpanda, P.; Recham, N.; Chotard, J.N.; Djellab, K.; Walker, W.; Armand, M.; Tarascon, J.M. Structure and electrochemical properties of novel mixed Li(Fe1−xMx)SO_4F (M = Co, Ni, Mn) phases fabricated by low temperature ionothermal synthesis. *J. Mater. Chem.* **2010**, *20*, 1659–1668. [CrossRef]
143. Otsuki, T.; Nonaka, N.; Takashima, W.; Qian, A.; Ishihara, T.; Imai, T.; Kabe, T. Oxidative Desulfurization of Light Gas Oil and Vacuum Gas Oil by Oxidation and Solvent Extraction. *Energy Fuels* **2000**, *14*, 1232–1239. [CrossRef]
144. Ramos, J.M.; Wang, J.A.; Flores, S.O.; Chen, L.F.; Nava, N.; Navarrete, J.; Domínguez, J.M.; Szpunar, J.A. Ultrasound-assisted synthesis and catalytic activity of mesostructured FeOx/ SBA-15 and FeOx/Zr-SBA-15 catalysts for the oxidative desulfurization of model diesel. *Catal. Today* **2018**. [CrossRef]
145. Rodríguez-Reinoso, F. The role of carbon materials in heterogeneous catalysis. *Carbon* **1998**, *36*, 159–175. [CrossRef]
146. Serp, P.; Figueiredo, J.L. *Carbon Materials for Catalysis*; John Wiley & Sons Inc.: Hoboken, NJ, USA, 2009.
147. Tharamani, C.N.; Bordoloi, A.; Schuhmann, W.; Muhler, M. Mesoporous nitrogen-rich carbon materials as catalysts for the oxygen reduction reaction. *ChemSusChem* **2012**, *5*, 637–641.
148. Su, F.C.; Mathew, S.; Lipner, G.; Fu, X.; Antonietti, M.; Blechert, S.; Wang, X. mpg-C3N4-Catalyzed Selective Oxidation of Alcohols Using O_2 and Visible Light. *J. Am. Chem. Soc.* **2010**, *132*, 16299–16301. [CrossRef] [PubMed]
149. Piccinino, D.; Abdalghani, I.; Botta, G.; Crucianelli, M.; Passacantando, M.; Di Vacri, M.L.; Saladino, R. Preparation of wrapped carbon nanotubes poly(4-vinylpyridine)/MTO based heterogeneous catalysts for the oxidative desulfurization (ODS) of model and synthetic diesel fuel. *Appl. Catal. B Environ.* **2017**, *200*, 392–401. [CrossRef]
150. Jin, X.; Balasubramanian, V.V.; Selvan, S.T.; Sawant, D.P.; Chari, M.A.; Lu, G.Q.; Vinu, A. Highly ordered mesoporous carbon nitride nanoparticles with high nitrogen content: A metal-free basic catalyst. *Angew. Chem. Int. Ed.* **2009**, *48*, 7884–7887. [CrossRef]
151. Goyal, R.; Sarkar, B.; Lucus, N.; Bordoloi, A. Acid–Base Cooperative Catalysis over Mesoporous Nitrogen-Rich Carbon. *ChemCatChem* **2014**, *6*, 3091–3095. [CrossRef]
152. Li, X.; Huang, S.; Xu, Q.; Yang, Y. Preparation of WO_3-SBA-15 mesoporous molecular sieve and its performance as an oxidative desulfurization catalyst. *Transit. Met. Chem.* **2009**, *34*, 943–947. [CrossRef]
153. Wang, H.; Gong, Y.; Wang, Y. Cellulose-based hydrophobic carbon aerogels as versatile and superior adsorbents for sewage treatment. *RSC Adv.* **2014**, *4*, 45753. [CrossRef]
154. Zhang, P.; Wang, Y.; Li, H.; Antonietti, M. Metal-free oxidation of sulfides by carbon nitride with visible light illumination at room temperature. *Green Chem.* **2012**, *14*, 1904–1908. [CrossRef]
155. Goyal, R.; Dumbre, D.; Sivakumar Konathala, L.N.; Pandey, M.; Bordoloi, A. Oxidative coupling of aniline and desulfurization over nitrogen rich mesoporous carbon. *Catal. Sci. Technol.* **2015**, *5*, 3632–3638. [CrossRef]
156. Wang, X.; Wu, J.; Zhao, M.; Lv, Y.; Li, G.; Hu, C.J. Partial Oxidation of Toluene in CH_3COOH by H_2O_2 in the Presence of VO $(acac)_2$ Catalyst. *J. Phys. Chem. C* **2009**, *113*, 14270–14278. [CrossRef]
157. Nair, S.; Tatarchuk, B.J. Supported silver adsorbents for selective removal of sulfur species from hydrocarbon fuels. *Fuel* **2010**, *89*, 3218–3225. [CrossRef]
158. Samokhvalov, A.; Duin, E.C.; Nair, S. Study ofthe surface chemical reactions of thiophene with Ag/titania by the complementary temperature-programmed electron spin resonance, temperature-programmed desorption, and X-ray photoelectron spectroscopy: Adsorption, desorption, and sorbent regeneration mechanisms. *J. Phys. Chem. C* **2010**, *114*, 4075–4085.
159. Mckinley, S.G.; Angelici, R.J. Deep desulfurization by selective adsorption of dibenzothiophenes on Ag+/SBA-15 and Ag+/SiO_2. *Chem. Commun.* **2003**, 2620–2621. [CrossRef]
160. Xiao, J.; Li, Z.; Liu, B. Adsorption of benzothiophene and dibenzothiophene on ion-impregnated activated carbons and ion-exchanged Y zeolites. *Energy Fuels* **2008**, *22*, 3858–3863. [CrossRef]
161. Xiao, J.; Bian, G.A.; Zhang, W.; Li, Z. Adsorption of dibenzothiophene on Ag/Cu/ Fe-supported activated carbons prepared by ultrasonic-assisted impregnation. *J. Chem. Eng.* **2010**, *55*, 5818–5823. [CrossRef]
162. Ghosh, S.; Acharyya, S.S.; Tiwari, R.; Sarkar, B.; Singha, R.K.; Pendem, C.; Sasaki, T.; Bal, R. Selective Oxidation of Propylene to Propylene Oxide over Silver-Supported Tungsten Oxide Nanostructure with Molecular Oxygen. *ACS Catal.* **2014**, *4*, 2169–2174. [CrossRef]

163. Hosseini, S.M.; Hosseini-Monfared, H.; Abbasi, V.; Khoshroo, M.R. Selective oxidation of hydrocarbons under air using recoverable silver ferrite–graphene ($AgFeO_2$–G) nanocomposite: A good catalyst for green chemistry. *Inorg. Chem. Commun.* **2016**, *67*, 72–79. [CrossRef]
164. Fellah, M.F.; Santen, R.A.; Onal, I. Epoxidation of ethylene by silver oxide (Ag_2O) cluster: A density functional theory study. *Catal. Lett.* **2011**, *141*, 762–771. [CrossRef]
165. Zhang, J.; Li, Y.; Zhang, Y. Effect of support on the activity of Ag-based catalysts for formaldehyde oxidation. *Sci. Rep.* **2015**, *5*, 12950. [CrossRef] [PubMed]
166. Li, Y.; Zhang, X.; He, H.; Yu, Y.; Yuan, T.; Tian, Z.; Wang, J.; Li, Y. Effect of the pressure on the catalytic oxidation of volatile organic compounds over Ag/Al_2O_3 catalyst. *Appl. Catal. B Environ.* **2009**, *89*, 659–664. [CrossRef]
167. Zhang, X.; Qu, Z.; Li, X.; Wen, M. Studies of silver species for low-temperature CO oxidation on Ag/SiO_2 catalysts. *Sep. Purif. Technol.* **2010**, *72*, 395–400. [CrossRef]
168. Ye, F.; Miao, G.; Wu, L.; Wu, Y.; Li, Z.; Song, C.; Xiao, J. [O]-induced reactive adsorptive desulfurization of liquid fuel over Ag X O@SBA-15 under ambient conditions. *Chem. Eng. Sci.* **2017**, *168*, 225–234. [CrossRef]
169. Dellasega, D.; Facibeni, A.; Fonzo, F.D. Nanostructured Ag_4O_4 films with enhanced antibacterial activity. *Nanotechnology* **2008**, *19*, 475602. [CrossRef] [PubMed]
170. Waterhouse, G. Influence of catalyst morphology on the performance of electrolytic silver catalysts for the partial oxidation of methanol to formaldehyde. *Appl. Catal. A Gen.* **2004**, *266*, 257–273. [CrossRef]
171. Derouin, J.; Farber, R.G.; Heslop, S.L.; Killelea, D.R. Formation of surface oxides and Ag2O thin films with atomic oxygen on Ag(111). *Surf. Sci.* **2015**, *641*, L1–L4. [CrossRef]
172. Car, P.-E.; Patzke, G.R. The Fascination of Polyoxometalate Chemistry. *Inorganics* **2015**, *3*, 511–515. [CrossRef]
173. Wang, S.-S.; Yang, G.-Y. Recent Advances in Polyoxometalate-Catalyzed Reactions. *Chem. Rev.* **2015**, *115*, 4893–4962. [CrossRef]
174. Ammam, M. Polyoxometalates: Formation, structures, principal properties, main deposition methods and application in sensing. *J. Mater. Chem. A* **2013**, *1*, 6291–6312. [CrossRef]
175. Omwoma, S.; Gore, C.T.; Ji, Y.; Hu, C.; Song, Y.-F. Environmentally benign polyoxometalate materials. *Coord. Chem. Rev.* **2015**, *286*, 17–29. [CrossRef]
176. Narasimharao, K.; Brown, D.R.; Lee, A.F.; Newman, A.D.; Siril, P.F.; Tavener, S.J.; Wilson, K. Structure–activity relations in Cs-doped heteropoly acid catalysts for biodiesel production, *J. Catal.* **2007**, *248*, 226–234. [CrossRef]
177. Contreras Coronel, N.; da Silva, M.J. Lacunar Keggin Heteropolyacid Salts: Soluble, Solid and Solid-Supported Catalysts. *J. Clust. Sci.* **2018**, *29*, 195–205. [CrossRef]
178. Lotfian, N.; Heravi, M.M.; Mirzaei, M.; Heidari, B. Applications of inorganic-organic hybrid architectures based on polyoxometalates in catalyzed and photocatalyzed chemical transformations. *Appl. Organomet. Chem.* **2019**, *33*, 4808. [CrossRef]
179. Ye, J.-J.; Wu, C.-D. Immobilization of polyoxometalates in crystalline solids for highly efficient heterogeneous catalysis. *Dalton Trans.* **2016**, *45*, 10101–10112. [CrossRef]
180. Dufaud, V.; Lefebvre, F. Inorganic Hybrid Materials with Encapsulated Polyoxometalates. *Materials* **2010**, *3*, 682–703. [CrossRef]
181. Hossain, M.N.; Park, H.C.; Choi, H.S. A Comprehensive Review on Catalytic Oxidative Desulfurization of Liquid Fuel Oil. *Catalysts* **2019**, *9*, 229. [CrossRef]
182. Yan, X.; Yan, J.; Mei, P.; Lei, J. Synthesis, characterization and catalytic properties of mesoporous $HPMo/SiO_2$ composite. *J. Wuhan Univ. Technol.* **2008**, *23*, 834–838. [CrossRef]
183. Yan, X.; Lei, J.; Liu, D.; Guo, L.; Wu, Y. Oxidation reactivities of organic sulfur compounds in fuel oil using immobilized heteropoly acid as catalyst. *J. Wuhan Univ. Technol.* **2007**, *22*, 320–324. [CrossRef]
184. Kaleta, W.; Nowinska, K. Immobilisation of Heteropoly Anions in Si-MCM-41 Channels by Means of Chemical Bonding to Aminosilane Groups. *Chem. Commun.* **2001**, 535–536. [CrossRef]
185. Wang, S.-Q.; Zhou, L.; Su, W.; Sun, Y.; Zhou, Y. Deep Desulfurization of Transportation Fuels by Characteristic Reaction Resided in Adsorbents. *AIChE J.* **2009**, *55*, 1872–1881. [CrossRef]
186. Li, J.; Hu, B.; Tan, J.; Zhuang, J. Deep oxidative desulfurization of fuels catalyzed by molybdovanadophosphoric acid on amino-functionalized SBA-15 using hydrogen peroxide as oxidant. *Transit. Met. Chem.* **2013**, *38*, 495–501. [CrossRef]

187. Chamack, M.; Mahjoub, A.R.; Aghayan, H. Catalytic performance of vanadium-substituted molybdophosphoric acid supported on zirconium modified mesoporous silica in oxidative desulfurization. *Chem. Eng. Res. Des.* **2015**, *94*, 565–572. [CrossRef]
188. Wang, X.; Zhang, X.; Wang, Y.; Liu, H.; Qiu, J.; Wang, J.; Han, W.; Yeung, K.L. Investigating the role of zeolite nanocrystal seeds in the synthesis of mesoporous catalysts with zeolite wall structure. *Chem. Mater.* **2011**, *23*, 4469–4479. [CrossRef]
189. Chamack, M.; Mahjoub, A.R.; Aghayan, H. Cesium salts of tungsten-substituted molybdophosphoric acid immobilized onto platelet mesoporous silica: Efficient catalysts for oxidative desulfurization of dibenzothiophene. *Chem. Eng. J.* **2014**, *255*, 686–694. [CrossRef]
190. Trakarnpruk, W.; Jatupisarnpong, J. Acidic and cesium salts of polyoxometalates with and without vanadium supported on MCM-41 as catalysts for oxidation of cyclohexane with H_2O_2. *Appl. Petrochem. Res.* **2013**, *3*, 9–15. [CrossRef]
191. Torres-Garcia, E.; Galano, A.; Rodriguez-Gattorno, G. Oxidative desulfurization (ODS) of organosulfur compounds catalyzed by peroxo-metallate complexes of WO_x–ZrO_2: Thermochemical, structural, and reactivity indexes analyses. *J. Catal.* **2011**, *282*, 201–208. [CrossRef]
192. Zhuang, J.; Jin, X.; Shen, X.; Tan, J.; Nie, L.; Xiong, J.; Hu, B. Preparation of Ionic Liquid-modified SBA-15 Doped with Molybdovanadophosphoric Acid for Oxidative Desulfurization. *Bull. Korean Chem. Soc.* **2015**, *36*, 1784–1790. [CrossRef]
193. Xiong, J.; Zhu, W.; Ding, W.; Yang, L.; Zhang, M.; Jiang, W.; Zhao, Z.; Li, H. Hydrophobic mesoporous silica-supported heteropolyacid induced by ionic liquid as a high efficiency catalyst for the oxidative desulfurization of fuel. *RSC Adv.* **2015**, *5*, 16847–16855. [CrossRef]
194. Cai, T.-F.; Li, H.-P.; Zhao, H. A Study on the Oxidation-extraction Desulfurization of FCC Gasoline Over Supported Phosphotungstic Acid/H_2O_2/Dimethyl Sulfoxide (DMSO). *Pet. Sci. Technol.* **2014**, *32*, 1713–1719. [CrossRef]
195. Yang, L.; Li, J.; Yuan, X.; Shen, J.; Qi, Y. One step non-hydrodesulfurization of fuel oil: Catalyzed oxidation adsorption desulfurization over HPWA-SBA-15. *J. Mol. Catal. A* **2007**, *262*, 114–118. [CrossRef]
196. Estephane, G.; Lancelot, C.; Blanchard, P.; Toufaily, J.; Hamiye, T.; Lamonier, C. Sulfur compounds reactivity in the ODS of model and real feeds on W–SBA based catalysts. *RSC Adv.* **2018**, *8*, 13714–13721. [CrossRef]
197. Dai, W.; Zhou, Y.; Wang, S.; Long, L.; Zhou, L. Catalytic Oxidation of Thiophenes with Air and PW/SBA-15. *Ads. Sci. Technol.* **2007**, *25*, 385–394. [CrossRef]
198. Lu, C.; Fu, H.; Li, H.; Zhao, H.; Cai, T. Oxidation-extraction desulfurization of model oil over Zr-ZSM-5/SBA-15 and kinetic study. *Front. Chem. Sci. Eng.* **2014**, *8*, 203–211. [CrossRef]
199. Qi, H.-X.; Zhai, S.-R.; Zhang, W.; Zhai, B.; An, Q.-D. Recyclable HPW/PEHA/ZrSBA-15 toward efficient oxidative desulfurization of DBT with hydrogen peroxide. *Catal. Commun.* **2015**, *72*, 53–56. [CrossRef]
200. Lei, J.; Chen, L.; Yang, P.; Du, X.; Yan, X. Oxidative desulfurization of diesel fuel by mesoporous phosphotungstic acid/SiO_2: The effect of preparation methods on catalytic performance. *J. Porous Mater.* **2013**, *20*, 1379–1385. [CrossRef]
201. Ribeiro, S.O.; Granadeiro, C.M.; Almeida, P.L.; Pires, J.; Capel-Sanchez, M.C.; Campos-Martin, J.M.; Gago, S.; de Castro, B.; Balula, S.S. Oxidative desulfurization strategies using Keggin-type polyoxometalate catalysts: Biphasic versus solvent-free systems. *Catal. Today* **2019**, *333*, 226–236. [CrossRef]
202. Ribeiro, S.O.; Nogueira, L.S.; Gago, S.; Almeida, P.L.; Corvo, M.C.; de Castro, B.; Granadeiro, C.M.; Balula, S.S. Desulfurization process conciliating heterogeneous oxidation and liquid extraction: Organic solvent or centrifugation/water? *Appl. Catal. A* **2017**, *542*, 359–367. [CrossRef]
203. Pham, X.N.; Tran, D.L.; Pham, T.D.; Nguyen, Q.M.; van Thi, T.T.; Van, H.D. One-step synthesis, characterization and oxidative desulfurization of 12-tungstophosphoric heteropolyanions immobilized on amino functionalized SBA-15. *Adv. Powder Technol.* **2018**, *29*, 58–65. [CrossRef]
204. Pham, X.N.; van Doan, H. Activity and stability of amino-functionalized SBA-15 immobilized 12-tungstophosphoric acid in the oxidative desulfurization of a diesel fuel model with H_2O_2. *Chem. Eng. Commun.* **2019**, *206*, 1139–1151. [CrossRef]
205. Zhang, Y.; Wu, L.; Dong, X.; Wu, P.; Hu, H.; Xue, G. Copper(II)-Substituted Polyoxotungstates Immobilized on Amine-Functionalized SBA-15: Efficient Heterogeneous Catalysts for Liquid Phase Oxidative Reaction. *Catal. Lett.* **2016**, *146*, 2468–2477. [CrossRef]

206. Julião, D.; Mirante, F.O.; Ribeiro, S.O.; Gomes, A.C.; Valença, R.; Ribeiro, J.C.; Pillinger, M.; de Castro, B.; Gonçalves, I.S.; Balula, S.S. Deep oxidative desulfurization of diesel fuels using homogeneous and SBA-15-supported peroxophosphotungstate catalysts. *Fuel* **2019**, *241*, 616–624. [CrossRef]
207. Ribeiro, S.O.; Duarte, B.; de Castro, B.; Granadeiro, C.M.; Balula, S.S. Improving the Catalytic Performance of Keggin $[PW_{12}O_{40}]^{3-}$ for Oxidative Desulfurization: Ionic Liquids versus SBA-15 Composite. *Materials* **2018**, *11*, 1196. [CrossRef] [PubMed]
208. Yuan, J.; Xiong, J.; Wang, J.; Ding, W.; Yang, L.; Zhang, M.; Zhu, W.; Li, H. Structure and catalytic oxidative desulfurization properties of SBA-15 supported silicotungstic acid ionic liquid. *J. Porous Mater.* **2016**, *23*, 823–831. [CrossRef]
209. Xiong, J.; Zhu, W.; Ding, W.; Yang, L.; Chao, Y.; Li, H.; Zhu, F.; Li, H. Phosphotungstic Acid Immobilized on Ionic Liquid-Modified SBA-15: Efficient Hydrophobic Heterogeneous Catalyst for Oxidative Desulfurization in Fuel. *Ind. Eng. Chem. Res.* **2014**, *53*, 19895–19904. [CrossRef]
210. Wang, L.; Fan, J.; Tian, B.; Yang, H.; Yu, C.; Tu, B.; Zhao, D. Synthesis and characterization of small pore thick-walled SBA-16 templated by oligomeric surfactant with ultra-long hydrophilic chains. *Microporous Mesoporous Mater.* **2004**, *67*, 135–141. [CrossRef]
211. Zhao, D.; Huo, Q.; Feng, J.; Chmelka, B.F.; Stucky, G.D. Nonionic Triblock and Star Diblock Copolymer and Oligomeric Surfactant Syntheses of Highly Ordered, Hydrothermally Stable, Mesoporous Silica Structures. *J. Am. Chem. Soc.* **1998**, *120*, 6024–6036. [CrossRef]
212. Gallo, J.M.R.; Bisio, C.; Marchese, L.; Pastore, H.O. Surface acidity of novel mesostructured silicas with framework aluminum obtained by SBA-16 related synthesis. *Microporous Mesoporous Mater.* **2008**, *111*, 632–635. [CrossRef]
213. Shah, A.T.; Li, B.; Ali Abdalla, Z.E. Direct synthesis of Ti-containing SBA-16-type mesoporous material by the evaporation-induced self-assembly method and its catalytic performance for oxidative desulfurization. *J. Colloid Interface Sci.* **2009**, *336*, 707–711. [CrossRef]
214. Boccuti, M.R.; Rao, K.M.; Zecchina, A.; Leofanti, G.; Petrini, G. Spectroscopic Characterization of Silicalite and Titanium-Silicalite. *Stud. Surf. Sci. Catal.* **1989**, *48*, 133–144.
215. Araújo, R.S.; Azevedo, D.C.S.; Rodríguez-Castellón, E.; Jiménez-López, A.; Cavalcante, C.L. Al and Ti-containing mesoporous molecular sieves: Synthesis, characterization and redox activity in the anthracene oxidation. *J. Mol. Catal. A Chem.* **2008**, *281*, 154–163. [CrossRef]
216. Eimer, G.A.; Chanquia, C.M.; Sapag, K.; Herrero, E.R. The role of different parameters of synthesis in the final structure of Ti-containing mesoporous materials. *Microporous Mesoporous Mater.* **2008**, *116*, 670–676. [CrossRef]
217. Zepeda, T.A. Comparison and performance of different sulphided Ti-loaded mesostructured silica-supported CoMo catalysts in deep HDS. *Appl. Catal. A* **2008**, *347*, 148–161. [CrossRef]